Ultrasound Sensing of Muscles for Prosthetic Control

A Major Qualifying Project

Submitted to the faculty of

WORCESTER POLYTECHNIC INSTITUTE

Worcester, MA

In partial fulfillment of the requirements for the degree of Bachelor of Science

Submitted by:

Mitch Gaines, Sebastian Hamori and Kenia Valdivia

Submitted on:

May 13th, 2020

Advised by:

Professor Haichong (Kai) Zhang
Professor Gregory Fischer

Abstract

Amputation in the arm results in decreased capability for individuals to manipulate their surroundings effectively. Advances in active prostheses have sought to augment these individuals with a prosthetic that returns some, but ideally all, functionality back to the individual. Specifically, in transradial amputations, many of the muscles required to move the hand are still intact. Sensors such as EMGs exist to provide information on the muscles located directly beneath the skin. However, the data they can provide is limited by muscle placement and their susceptibility to crosstalk and signal attenuation. Ultrasound can be used to produce a cross-sectional image of the forearm and the muscles present. Through the utilization of ultrasound images, assessments can be made on the muscles state and their effect on the downstream finger movements. Building off prior work done in this field, this project aims to demonstrate use of ultrasound in prosthetic control. To accomplish this, we designed and analyzed a prosthetic design to implement this technology, built the prosthetic, and performed an assessment on the optimal probe orientation on the forearm. It was indicated through our study that the optimal probe orientation on the forearm was a 90° placement as opposed to a 45° placement. With the outcomes of this project, it was proven that ultrasound sensing can be used for prosthetic control.

Acknowledgments

Worcester Polytechnic Institute

Advisors: Dr. Haichong Zhang & Dr. Gregory Fischer

Thank you to Dr. Christopher Nycz, Jakub Kamiński, & Yichuan Tang for supporting our project endeavors and providing ample assistance, feedback, and guidance whenever necessary.

Table of Contents

Chapter 1: Introduction

Current industry prostheses serve an important purpose to amputees, allowing these individuals to regain a functioning limb. This provides the opportunity of regaining a sense of normalcy following a traumatic event. Protheses help individuals continue their activities of daily living. Not only do they allow many people to hold and lift objects, but they are also used to prevent themselves from falling, for driving, for working and for cosmetic purposes.

The prosthetic industry ranges from some protheses being merely cosmetic to more advanced options such as body-powered systems. Further, prostheses exist that use electromyography (EMG) technology to utilize electrical signals and translate them to the movements of the prosthetic limb. EMG prostheses can correlate the firing of muscles to the movement of the artificial limb like flipping a light switch. These systems are presented with a few inherent limitations, however. First, EMG sensors are designed such that they need to be placed either on the surface of the skin or within reach of a probe that is placed directly beneath the skin. Access to muscles located any further beneath the skin is not feasible. Further, EMGs are highly susceptible to crosstalk and signal attenuation. This makes them highly problematic when used for applications requiring signal consistency, such as machine learning.

B-mode ultrasound constructs a two-dimensional image based on the depth of obstructions beneath the skin. Obstructions include muscle fibers and bones which reflect the signal. Intensity of the reflected signal is processed and is displayed as a grayscale value ranging from 0-255. B-mode probes consist of multiple channels that make up the transducer. These signals are produced and processed in parallel with one another. This allows for a field of view to be created showing the intensity at varying depths across a wider region (Koundal, 2019).

This project implements the use of ultrasound technology in muscle sensing and prosthetic control. Because ultrasound sensing provides more depth and precision than the standard EMG, this project aims to prove the use of ultrasound in prosthetic design for more precise control of hand prostheses. Specifically, our team focused on finger control through the sensing of muscle firing in the mid-forearm. Ultrasound was used to analyze changes in hand states. Our team laid the groundwork for a more robust demonstration of ultrasound use in prosthesis to be pursued. Data was collected using a synchronized ultrasound machine and a motion capture system. In simulation, it can demonstrate respective hand motions from an ultrasound image input as well as move the fingers of the prosthetic to their respective positions. A prosthetic hand was designed and developed for demonstration purposes and is modelled after the control in the simulation. Additionally, an in-depth analysis was done for the proper probe orientation on the forearm with respect to the prosthetic.

Chapter 2: Background

2.1 Prosthetic Application and Design

2.1.1 Anatomy of the Hand

The hand functions as a tactical organ that humans use to interact with and influence their surroundings. It is composed of 38 bones that connect to the wrist, which is composed of 18 bones. Of the 38 hand bones, they are composed of 10 metacarpal bones and 28 phalanges (Jr, William, 2018). The 28 phalange bones consist of the index, middle, ring and little fingers distal, middle and proximal phalanges and the distal and proximal phalanges of the thumb.

Controlling the movement of the hand's phalanges and metacarpals are 34 unique muscles located across the forearm and palm. The muscles used to control the hand are divided into two groups with extrinsic and intrinsic muscles. Intrinsic muscles are located on the hand itself whereas the extrinsic are located on the forearm (Jones, 2018). Extrinsic muscles are divided into four major groups: anterior flexors, the posterior extensors, the lateral extensors-supinator, and medial flexor-pronators. Flexors and extensors are responsible for the control of individual digits that give rise to tendons. In the flexion of the proximal and distal interphalangeal joints, the body uses the flexor digitorum profundus (FDP) and flexor digitorum superficialis (FDS). The digits that are relevant to these main muscles are the index, middle, ring and pinky finger. The thumb is controlled by the flexor pollicis longus (FPL), extensor pollicis longus, and abductor pollicis longus (N. Akhlaghi, 2016).

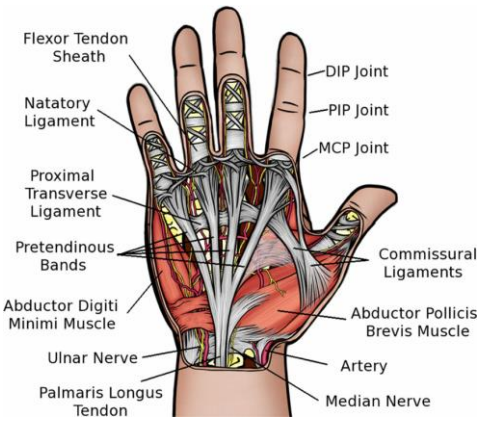

Figure 1: Internal Hand Mechanics (Cabibihan, 2014)

Tendons in the hand are covered by a tendon sheath which separates the tendons from the rest of the hand and supports its unique stretching and movement patterns. Fig. 1 shows the internal layout within an individual hand including labels showing the many joints, tendons, tendon sheath, muscles and some of the other mechanisms that support the hand.

2.1.2 Prosthetic Designs Choices

Amputations can be defined under one of four levels: transtibial, transfemoral, transradial, and transhumeral. Prostheses are designed to accompany each of these respective amputation types as well as

account with variability in sizing of attachment to the stump. These prostheses can fall into one of two categories: active and passive. Passive prostheses are generally cosmetic in nature and their actuation is, generally, limited in its capabilities. Active prosthetics are prosthetic limbs that use systems of motors and electronics to accomplish actuation (Prostheses, 2019). Actuation with these systems can either be performed independently of muscles by using some external control, or integration into the muscles. Sensing of the muscles can be done using electromyography (EMG), or in our case, ultrasound technology (Clements, 2019).

Design of prostheses are highly customizable. These customizations include things such as material selection and actuation capabilities. All these options contribute to the final cost of the system for the end user. Customization of prostheses is an important aspect of these systems, because of their high rate of rejection (Huinink, 2016). Users want a system that looks and feels natural. Body-powered systems are the most widely used because they are low in cost, relatively lightweight and durable. These prostheses are powered by a harness that is placed across the amputee's shoulder. Operation is performed by a system of cables that link the movement of the body to the prosthetic. Movement of the body helps the prosthetic perform its functions, including opening, closing and grasping.

Figure 2 Body Powered Hook (OttoBock, 2020)

Figure 3: Body-Powered Mechanical Hand (OttoBock, 2020)

2.2 Electromyography

Classic electromyography (EMG) technology involves the placement of electrodes underneath the skin and into a patient’s muscle. This allows for electrical activity to be monitored in the muscles. During muscle contraction, muscle fibers are activated and produce action potentials. Action potential is the result of a depolarization of the cell membranes. This results in a change in electric potential and causes adjacent cells to also depolarize, creating a wave of depolarization. Electric potential is then read by the electrodes placed in the muscles. Recent advancements have been made in EMG technology to allow for skin placement, meaning it can read electric potential without being placed in the muscle. Signals produced by EMGs can be used for a widespread use of research applications. These applications include

the diagnosis of neuromuscular abnormalities (Johns Hopkins Medicine, 2020) and use in wearable prostheses. Fig. 4 shows example outputs from an EMG placed on the forearm and performing various movements of the wrist and fingers.

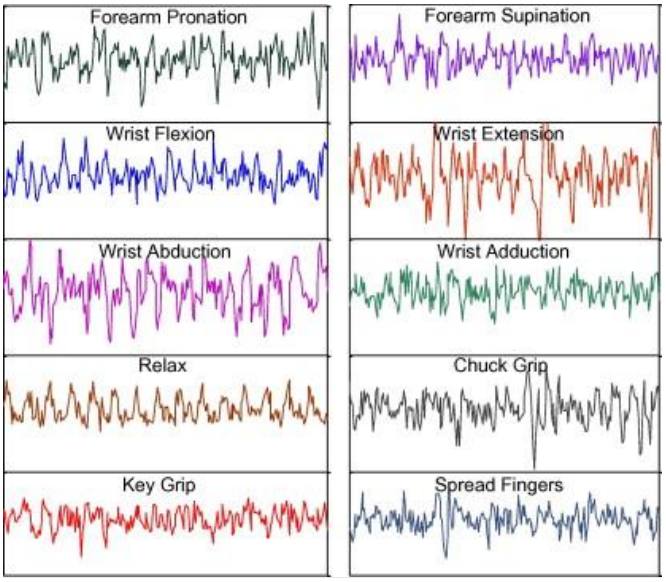

Figure 4: Example EMG output from forearm extensor muscles (Rafiee, 2011)

2.2.1 EMG in Prosthetics

Prior work has been done to prove the use of this technology in these applications. In the case of individuals utilizing prostheses, the muscles required to move the downstream, but absent limbs, remain intact and functional for the most part. This is not the case, however, for individuals with neurodegenerative disorders such as Parkinson's. Because of the intact nature of the muscles and nervous system in amputee patients, EMGs can provide repeatable real time insights into the state of muscles. Motions of limbs can be interpolated from these signals (Sudarsan, 2020). Features of the signals produced from EMGs can be used to make inferences on the movements of the wrist and fingers. These have produced more accurate results than use of machine learning. These features can be extracted in a variety of methods. One of these methods includes placement of a matrix of sensors across an area (Rafiee, 2011). Transforms can then be used to extract features from the resultant signals. In an objective comparison, it was found that the discrete wavelet transform (DWT) worked the best amongst transforms and machine learning models at creating consistent features from EMG signals (Karlik, 2014).

While EMGs provide insights into when a muscle is being contracted, they are limited in a few aspects. First, they can only read signals of muscles sitting directly below the skin. This is inherently a limiting factor in their design. It provides good enough results in the case of lower-body prostheses, however, for reading intricate hand motions, they do not provide enough insights. Second, while

repeatable in short-term repetitive motions, over time, as muscles fatigue, the signal wears. Signal degradation as a result of fatigue is due to a decrease in action potential being produced by the muscles (Stock, 2020). Lastly, EMG signals are highly susceptible to crosstalk and signal attenuation. For use in prostheses where many of these would be used to accurately capture motion, their signals are not as repeatable or predictable as they need to in order to accurately describe intricate motions. In the case of hand prostheses, this is a major limiting factor.

2.3 Ultrasound Technology

Ultrasound operates by transmitting 1-5MHz sound pulses through a probe. These waves are reflected off of the edges of muscles and a distance and intensity is returned to the probe. Fig. 5 shows how this works. Using the data that is collected, an image can be constructed (Freudenrich, 2019). There are two relevant types of ultrasound probes with our project: A-Mode and B-Mode. A-Mode, often referred to as one-dimensional ultrasound, returns depth on the x-axis and amplitude on the y-axis. This allows the researcher to assess the muscles that contract at varying depths. B-Mode operates in a similar way. Amplitude across two dimensions is returned with corresponding variations in brightness relative to depth. Using both technologies, static and dynamic tracking of muscle contraction over time can be performed.

Ultrasound technology, sonomyography (SMG), is compared with EMG technology for use in detection of muscle contraction. While EMGs have their use cases, they are particularly susceptible to crosstalk and signal attenuation. Further, they can only measure binary values of whether or not a muscle directly below the skin where it is placed has contracted. SMGs allow for analog values of how contracted specific muscles are. Additionally, muscles that are not directly beneath the skin can be detected (T.W.S, 2016).

Through the application of ultrasound technology, information about muscle contraction, muscle thickness, and muscle location can be extracted (Guo, 2019). Images of these areas can then be placed into a machine learning model in order to produce expected outputs such as torque and joint flexion (Guo, 2019). Applications of this could include blood pressure monitoring, prosthetic control, exoskeleton control, and other similar applications. For all of these applications there is a need to have the probe supported in an orientation perpendicular to the surface and aiming at the target area. Manual support of the probe on the by an individual’s hand achieves this. In the prosthetic or exoskeleton control applications it is best to have the probe be supported on its own.

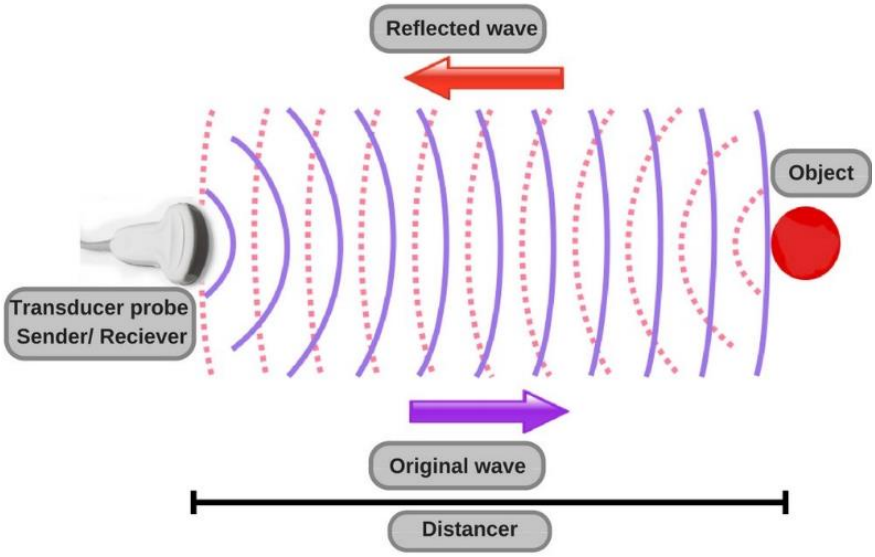

Figure 5: Ultrasound Probe Wave Transmission (Stock, 2020)

2.3.1 Hand Motions Using Ultrasound Imaging

Ultrasound imaging allows visualization of the cross-sectional anatomy of muscles. Real-time imaging can be used to track muscle contraction and relaxation. Through ultrasound imaging, the focus can be on the extrinsic flexor muscles. These flexors are visible through ultrasound imaging.

Several experiments have been performed analyzing the use of ultrasound imaging to classify hand motions. In the first experiment studied, the subjects perform fifteen different hand motions with seven repetitions. Activities patterns were evaluated through imaging. A second experiment had the subject perform different hand movements and results were controlled in real-time. Hand motions were classified and examined to see the accuracy of the hand movements. Another study dealt with evaluating graded control. Flexion of the fingers was tracked through a motion capture system. Markers were placed on the fingers and on the probe. The motion capture system was able to track the markers and the finger flexes. The final experiment was split to focus on a variation of the arm and forearm positions and variations of wrist positions. Patterns were evaluated with this study.

Individual finger flexion was generalized into more complex hand motions. A report of the motion pattern was generated. Through these experiments the classification accuracy was 91% and real-time imaged-based classification accuracy was 92%. The result showed how feasible it is to use ultrasound imaging for control of hand prosthesis (N. Akhlaghi, 2016).

Probe orientations were previously tested at a 90-degree angle in different experiments. Sikdar tested at mid forearm and Castellini tested at the wrist. Through Castellini's experiment he was able to estimate continuously changing finger motions through analyzing ultrasound images. (Castellini, 2011).

Sikdar's experiment focused on recognizing distinct hand gestures. They divided the image and calculated the average brightness change per region to create different activity patterns for each gesture. This resulted in classification of individual finger movements with a 98% accuracy. The result showed that with the ultrasound probe at a 90-degree angle there was a high accuracy in motion recognition. (Sikdar, 2014).

2.3.2 Combining Ultrasound Technology with Powered Systems

As mentioned, the use of ultrasound can be used to detect muscle contractions at varying depths underneath skin. Levels of contraction can be extracted from either RF data or image processing. Powered systems can then use this data in order to make intelligent decisions. Examples of powered systems that could be used are prostheses and musculoskeletal control devices, such as exoskeletons. When developing these devices, the behavior of existing muscles is an important aspect of their functionality. It was found that amputations, warranting the need for a prosthetic, usually do not inhibit muscle signal behavior. This is not the case for the population that would use a musculoskeletal control device. Muscle contractions become inconsistent in these cases and models detailing the data are difficult to infer (Nycz, 2019).

Prior work in prostheses has been pursued. Typically, this work focuses on one degree of freedom for motion in the hand. Machine learning models are used in order to convert the detected data into a corresponding motion. Simple support vector machines (SVM) and artificial neural networks (ANN) have yielded some success in this field. For example, estimation of wrist flexion angle has been studied through the use of ultrasound on the forearm. Using A-mode ultrasound and an SVM, yielded results with a p-value less than 0.02 (Hong-Bo, 2012). Similar work has been done to detect the opening and closing of fists. Data required to train these algorithms can be acquired by recording the images at every frame and synchronization with a motion capture system. This motion capture system is used to label the data being collected. These image data points allow the machine learning models to correlate image to motion which has shown to provide intuitive prosthetic response. This intuitive prosthetic response allows for the user to manipulate digits on the fly with a single required mode of use. (Ackerman, 2017).

Some prostheses are beginning to utilize ultrasound technology due to the reduction of noise and crosstalk which can as a result produce more accurate muscle response data. With this development, teams have found that the ANN have been able to better correlate fine muscle movement with this type of imaging. As a result, some prosthetics have begun to detect more precise muscle movements and then correlate them to the corresponding and desired prosthetic movements (Densford, 2017). Unfortunately, there is a lack of research into probe orientation for detection, which is something we decided to pursue within this project. Other groups are also pursuing the use of multiple ultrasound probes to produce 3D image results and even more accurate muscle movement data (Douglas, 2002).

Chapter 3: Methodology

Members of this project team each brought a diverse skill set based on their area of study. Because of this, the project was divided into independent, but reliant subsystems and pursued in parallel. Dependencies for each of the components were mapped out in Fig. 6. A few of the sub-components listed were pursued in adjacent projects that interact with the outcomes of this project. In Fig. 6, the process flow can be seen and how each step had dependencies and also influenced the steps that followed. Specifically, this project focused on the data collection, probe placement, prosthetic design, and simulation subcomponents. Some of these components have dependencies on machine learning and all have a dependency on data collection. However, the team had to consider the possibility that failures may occur in development. Risk assessment was performed to generate backup plans for each of the pursued subcomponents in the event that one of them was found to be inviable.

Supporting equipment used included the Verasonics ultrasound machine for all data collection performed in this project. For data collection, in addition to the Verasonics machine, the Vicon motion capture system was used. Using the data from these two systems, optimal probe placement on the forearm could be determined and machine learning models could be trained. These components influenced the mechanical design and the control of the prosthetic and simulation.

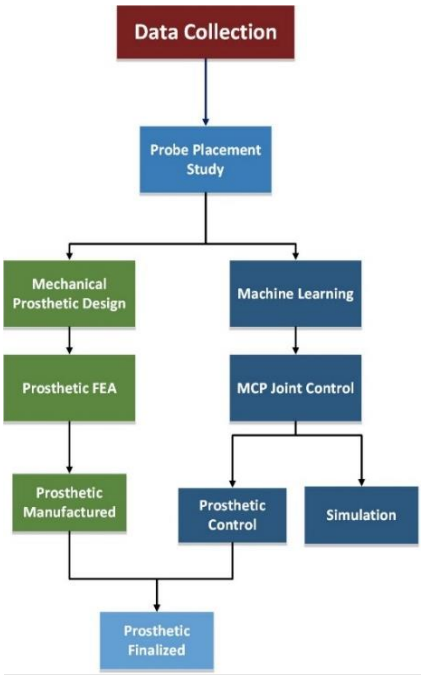

Figure 6: Project Process Flow Map

3.1 Probe Orientation

Extrinsic muscles located on the forearm are the muscles that control the hand. There are intrinsic muscles in the hand as well, much of the finger motion is controlled by the extrinsic muscles though. These muscles allow for wrist and finger movement. Extrinsic muscles can be categorized into flexor and extensor muscles which allows for bending and straightening of the fingers. Finger movements change the musculature of the forearm due to muscle contractions. Different finger movement changes the image the ultrasound displays.

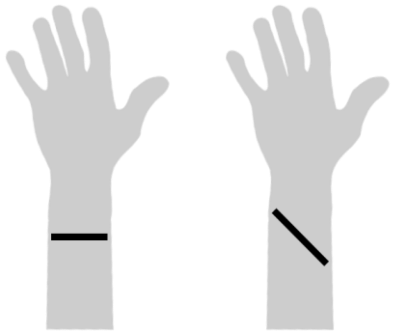

Figure 7: Orientation of the probe placement with palm facing up

In order to quantify probe orientation, two different locations are tested which are shown in Fig. 7. The ultrasound probe is first tested at a 90° angle with respect to the forearm, following the collection protocol: flexion of all fingers, fist and relaxed and the hand at stationary position. Data is collected on the same day to obtain precise results. The same procedure is followed for the 45° angle placement. Testing at a 90° angle has been used in prior work (Castelline, 2011 & Sidkar, 2014). The studies resulted in successful visualization of the muscles of the hand, these muscles consisting of the Flexor digitorum superficialis muscle and the Flexor digitorum. Therefore, it is hypothesized that the ultrasound probe placed at a 90° angle would produce a greater magnitude of muscle change than placing the ultrasound probe at a 45° angle (Castelline, 2011 & Sidkar, 2014).

This study is conducted on one test subject. Throughout the study, the team collected data that displayed ultrasound images that show muscle movements. Data is collected in frames where each frame correlates to an ultrasound image. During data collection the test subject has the elbow extended on a flat surface, with the forearm and hand supinated. Ultrasound gel is added to the mid forearm, then the probe is attached at a 90° throughout all the motions. Data is saved for each individual motion; therefore, it is much simpler to differentiate between motions. Next, the probe is then placed at a 45° angle and follows the same testing protocol. The data is then processed through MATLAB with the algorithms created.

3.1.1 Data Analysis

In order to track the magnitude of muscle change, three different analyses are performed. This analysis is done by creating three algorithms on MATLAB that would quantify muscle movement. As each frame analyzed correlates to an image, the difference between the hand being in a stationary position to flexion is shown in Figure 8 and 9.

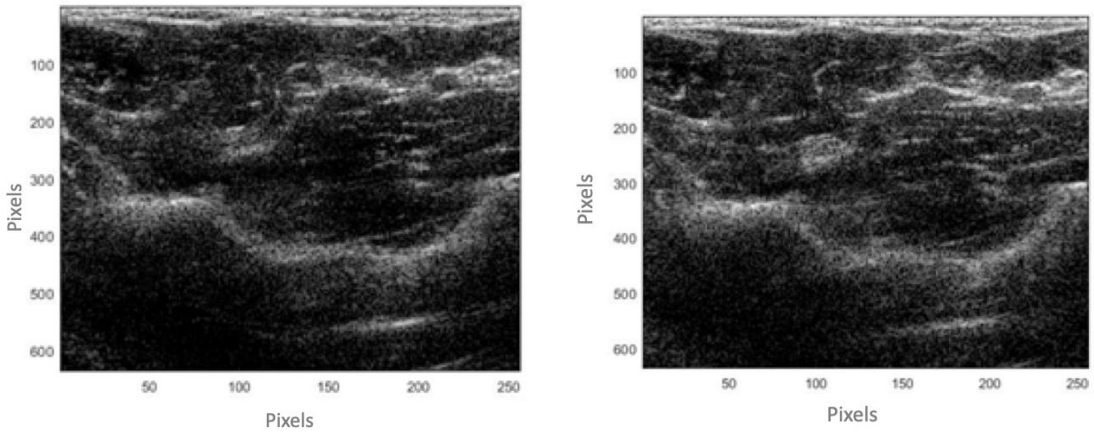

Figure 8: 90° angle of image at stationary position (on the left) and image of flexion (on the right)

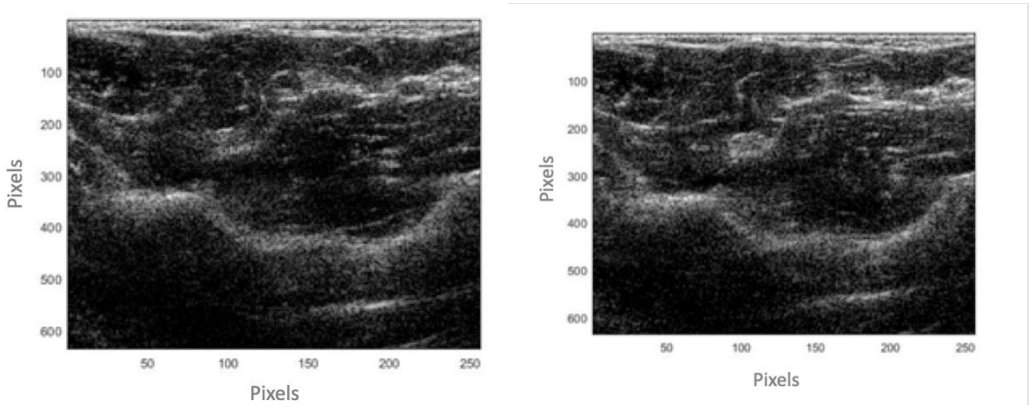

Figure 9: 45° angle of image at stationary position (on the left) and image of flexion (on the right)

The first two quantification analyses use cross-correlation to measure similarities of the two images as a function of displacement of one relative to another. MATLAB uses the equation in Figure 10 to determine the cross-correlation values.

The 2-D cross-correlation of an M-by-N matrix, X, and a P-by-Q matrix, H, is a matrix, C, of size $M+P-1$ by $N+Q-1$. Its elements are given by

$$C(k,l) = \sum_{m=0}^{M-1} \sum_{n=0}^{N-1} X(m,n)\,\overline{H}(m-k, n-l), \qquad \begin{aligned} -(P-1) &\le k \le M-1, \\ -(Q-1) &\le l \le N-1, \end{aligned}$$

where the bar over H denotes complex conjugation.

Figure 10: Cross Correlation Equation (MathWorks, 2020)

The first analysis performed is a consecutive image comparison. This algorithm allows for images to be compared to one another, therefore image one would be compared to image two, then two to three, three to four, etc. The second analysis uses an algorithm comparing the first image to all other images of their corresponding motion. These analyses are done for both orientations. Data obtained is processed in an excel sheet. This data is then graphed so that the team could identify the points where the flexions of

the motions occur. Valleys that are shown in the graph indicate a flexion. Once those points are identified, averages and standard deviations are calculated. Flexions are picked as the data points because the team wanted to analyze the magnitude of muscle change and this change would occur during flexions. Observed in Figures 11 and 12, the valleys of the graphs demonstrate the flexions of the thumb. Other flexions for each motion are also analyzed.

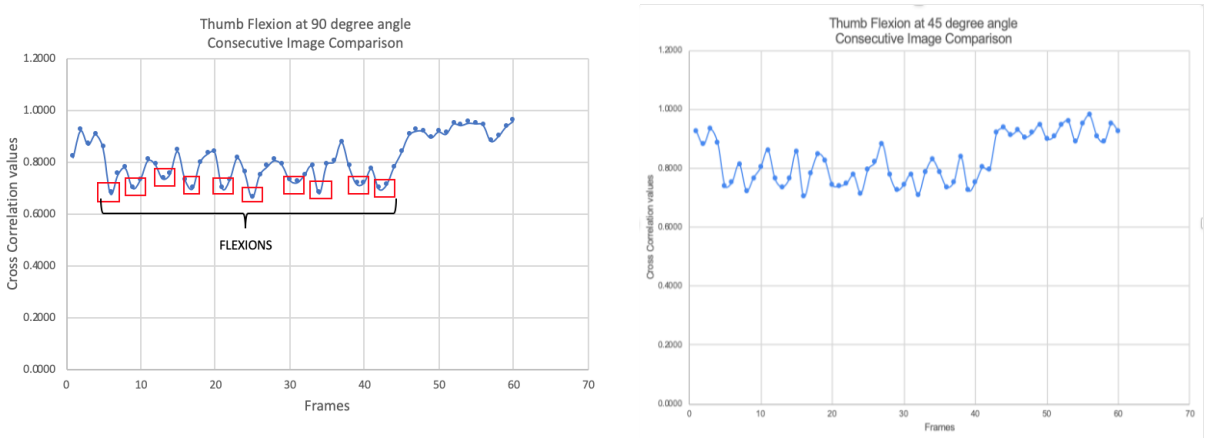

Figure 11: Graphs of Thumb flexion using consecutive image analysis

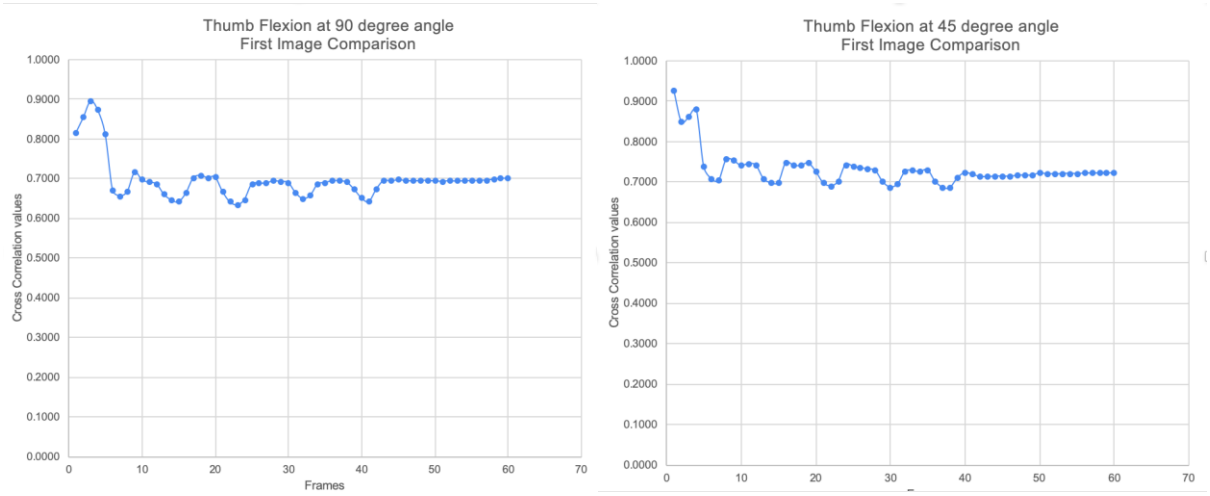

Figure 12: Graphs of Thumb flexion using first image analysis

The third analysis is image segmentation. Image segmentation is used to partition an image into regions, the regions are composed of pixels. The data used for this analysis is the same as the previous analysis; composed of files for each motion recorded. As each frame corresponds to an image, each image was 636x256 pixels. The algorithm created divides the images into eight even regions, dividing decibel data and computing 2D correlation coefficient for the image subregions overtime. The correlation results are then processed in an excel sheet. On the excel sheet the first row was labeled as either 90° or 45° and the row below was labeled by the specific motions separated by regions. Once the data is transferred from MATLAB to the excel sheet, the flexions for each motion are identified using the flexion from the

consecutive image analysis. Each of the flexions are represented by eight data points that correspond to a region shown in Fig. 13.

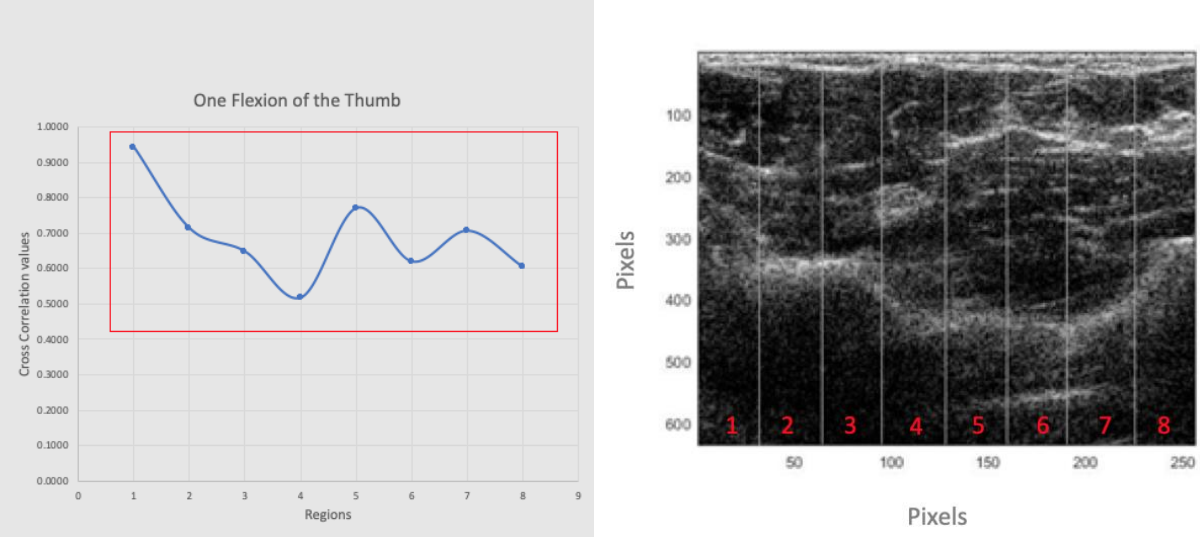

Figure 13: Close up of one flexion of the thumb at 90-degree angle divided into eight regions. (on the left), Ultrasound image split into 8 regions (on the right)

For each region the average of the cross-correlation coefficients and the standard deviations are calculated. The data is analyzed by comparing the eight regions of the 90° angle to its corresponding 45° angle for each motion flexion.

3.2 Prosthetic Design

With the prosthetic hands' significant impact on how user will interact with the world, it is very important to ensure it could complete the tasks required. Through background research and meetings as a team we discussed what the priorities should be in the design of the prosthetic. There are many prosthetic hands on the market that all have their own unique aspects so then next step was to determine which one of them would best fit our needs and what modifications would need to be made to optimize it for the user and our application. We also conducted a finite element analysis (FEA) to understand how this design would respond under possible loads. A major piece of making any prosthetic work is the interface with the user. In order to tackle this, we designed a gauntlet from scratch that would meet our priorities and interface with the prosthetic. Following that step, we began to focus on controlling the prosthetic. Based on prior experience and knowledge we compiled a list of priorities and then determined what parts would be ideal for our use. We proceeded by purchasing all parts required, manufacturing and assembling the prosthetic.

3.2.1 Design Requirements

To best determine the design requirements for the prosthetic, a weighted matrix was created. The contents of this matrix were determined through researching industry products and consumer reviews. A report with this information in detail can be found in Appendix C. Below is a table showing the weighted matrix.

			Material			Number of Joints		Movement System			Number of Motors	
Properties	Scaling Weights	ABS	Nylon	PLA	1	2	Linkage system	Cable system	3	4	All
Weight	7	5	5	5	5	4	5	5	3	4	5
Max Load	9	5	5	5	7	6	7	8	7	6	5
Range of Motion	9	5	5	5	5	9	5	5	10	8	8
Cost	6	6	8	5	6	5	5	6	1	3	5
Assembly Time	5	5	5	5	6	3	6	5	3	4	6
Durability	8	5	6	5	6	8	5	5	3	5	7
Manufacturing Time	5	5	5	5	5	8	8	5	5	5	5
Gripping Ability	9	5	7	6	6	7	5	5	7	6	5
Scalability	8	5	5	5	5	5	8	6	5	5	5
Cosmetics	6	5	5	5	3	5	5	7	5	5	5
Reliability	10	5	5	5	6	8	5	5	8	5	6
Serviceability	10	5	5	5	6	8	6	5	8	5	6
Total		466	**480**	468	**504**	481	476	**483**	465	465	**486**

Table 1: Prosthetic Design Weighted Matrix

With this matrix in mind, a list of design requirements was created. The list below includes many of the design requirements that were decided upon.

- Hand Material: Nylon
- Finger Joints: 2
- Motion System: Cable
- Number of Motors: 4
- Motion Pattern: Medial/Distal should angulate at same rate as proximal
- Desired Grasps Performed: Ball Grasp, Point, Fist, Open Palm

3.2.2 Base Design

From the findings with the weighted matrix, it was determined that the FlexyHand design was the best base design to work off of (Wood, 2014). Other designs reviewed included the Cyborg Beast, Talon Hand, Odysseus Hand, Raptor Hand, Dextrus Hand, Osprey Hand, Phoenix Hand, and K-1 Hand (Zuniga, 2014; Makerbot Thingverse: Talon Hand, 2014; Makerbot Thingverse: Odysseus Hand, 2014; Makerbot Thingverse: Raptor Hand, 2014; Makerbot Thingverse: Dextrus Hand, 2014; Makerbot Thingverse: Osprey Hand, 2015; Makerbot Thingverse: Phoenix Hand, 2016; K-1 Hand, 2015). This determination was made due to the design not being overly complex as it only requires one material for the hand construction, and it is designed to interact with a gauntlet which could include the motors to control the prosthetic. The design also functioned off of a cable system which was also an identified requirement. Fig. 14 is an image of the base design.

Figure 14: FlexyHand Prosthetic Design

3.2.3 Finite Element Analysis

Following the decision to use the FlexyHand design for our prosthetic hand, we validated that it will structurally be able to complete a sample task. In the ever-evolving age of technology, we decided to base this on the loads it will experience while typing. In order to validate this design, we had to design a new model finger so that it would accurately replicate the loading of the FlexyHand finger. This was done because the available model was not compatible with the SolidWorks simulation due to its format.

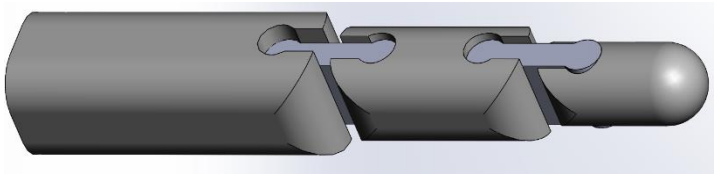

Figure 15: Model Finger

Following the creation of the model we had to create new materials in SolidWorks to ensure the simulation was accurate and reliable. Following that, we conducted a finite element analysis on the assembly with SolidWorks simulation. This analysis can be found in Appendix D. The loads that we tested were 500g, 1000g, and 1500g of force. We specifically investigated the part stress distribution (Kim, Jeong Ho 2012). Next, we compared the results to the material yield strength to ensure it would be able to withstand potential loads.

3.2.4 Gauntlet

This design lacked anything below the wrist which led us to designing a gauntlet to support the hand and any equipment required for its control. While producing the gauntlet we had a list of priorities to ensure it met our design requirements. Below is the list we used while designing:

- Similar geometry to human forearm
- External to internal cable routing
- Effective interface with FlexyHand prosthetic
- Can support the weight of hand and electronics
- Can support required equipment
- Interface with human is flexible and allows fastening for secure fit
- Is not heavier than human hand and forearm

Following the creation of that list, a quantifiable list was created to ensure that the specifications were met with the design. Below is the updated list:

- Geometry: 20-30.5cm long (Plagenhoef, S 1983)
- Cable routing external-internal
- Has Method of interfacing with two holes located at 2mm off center on FlexyHand design
- Structural Capacity: >1lb on platform
- Platform size: >8cm x 8cm
- Interface with human is flexible and allows fastening for secure fit
- Weight: <2.295lb (Zarzycka N 1989)

From this list of design specifications, iterations were created in SolidWorks with each one adding another modification ensuring all specifications are addressed. Another design aspect of the gauntlet is the implementation of an active grip. We pursued this idea and investigated possible solutions including a frictionless ring and a pivoting cylinder. This pivot point allows the prosthetic to grip a cylinder and sphere using the same control command. Below are images of the pivot point.

Figure 16: Low Friction Ring

(Universal Field Supplies, 2020)

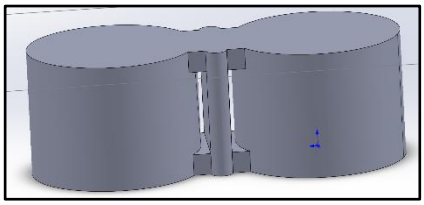

Figure 17: Active Grip Pivot

3.2.5 Electrical Components

Motors

In order to actuate the prosthetic and produce an accurate gripping force, we had to determine the motor that best fit our needs. The design considerations when making this decision were the loads required, price, size, and ease of use. Ultimately, a Pololu Micromotor with a 1000:1 gear ratio was used, as shown in Fig. 18.

Figure 18: Pololu Micromotor (Pololu Metal Gearmotor 1000:1, 2020)

Microcontroller

It was chosen to pursue development of the prosthetic with the ESP32 microcontroller. The ESP32 contained the necessary amount of PWM ports required for control of four motors. Power requirements for motor control were also well within the specifications supported by the microcontroller. Lastly, based on the experience of our team, the developer of the system has had experience using it. So, this microcontroller was the logical choice for development of the prosthetic.

Electronic Architecture

As shown in Fig. 19, the electronics architecture of the prosthetic consists of the ESP32 microcontroller, the motors, encoders for each motor, and a motor controller. For the microcontroller, the SN54410NE controller was used due to its compact size and its simple design. Additionally, in terms of sourcing of parts, this motor controller was available on campus. When connected to the microcontroller, the PWM outputs were connected to ports 2, 7, 10, and 15. Corresponding motor outputs were connected to ports 3, 6, 11, and 14.

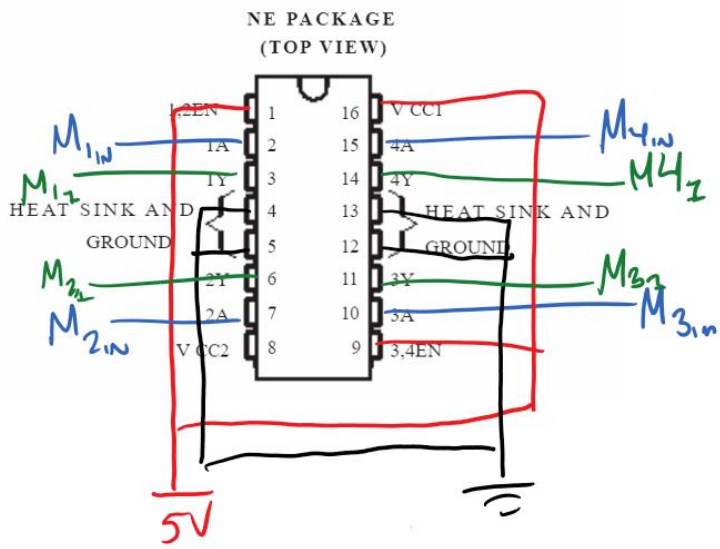

Figure 19: Circuit Design

3.3 Data Acquisition for Machine Learning Applications

Datasets are necessary for the application of machine learning algorithms that developed for this project. While it was not the specific focus of the project, many project dependencies rested on it. Data for this project was collected using the Verasonics ultrasound system. Using this system in conjunction with the Vicon motion capture system, data could be accurately labelled. To collect the quantity of data desired, a collection protocol was followed in order to streamline acquisition from subject to subject. Throughout the varying acquisitions, a probe attachment was required to be designed and manufactured to add placement consistency to the acquisitions.

3.3.1 Data Synchronization

The Verasonics ultrasound machine presented several challenges early in the project. One of these challenges included basic data collection from the machine. One aspect of this project was to collaborate with another ongoing MQP to develop a machine learning algorithm that could convert B-mode ultrasound images into five MCP joint outputs. For this to be possible, a huge amount of data was necessary. The ultrasound images collected required labels on them in order to train the machine learning model. Labels were acquired using a Vicon motion capture system.

Synchronization of these systems was required and presented much more difficulty than originally expected. The Verasonics system produces a synchronization signal in the form of a one microsecond pulse whenever a frame is captured. However, the Vicon system samples the synchronization signal at a rate of 1000 Hz. Because of this, a straightforward approach to

synchronization was not possible. In order to synchronize these systems, the output synchronization signal of the Verasonics machine was wired into an Arduino. Using an interrupt port to read the falling edge of the signal, a new signal was output with a 10-millisecond pulse. Output from the Arduino was connected to the analog input of the Vicon system. Frames from the Verasonics machine were then able to be later matched with associated frames from the Vicon system in post-processing.

3.3.2 Probe Attachment

In order to collect data, the ultrasound probe always had to be in contact with the forearm. This ensured that the results were consistent and reliable. The attachment supports the ultrasound probe and allows it to remain attached to the forearm without human contact. The attachment will also be able to change the orientation of the probe from a 90° angle to a 45° angle with respect to the forearm. Key factors that were considered while making the design included support, size, change of angles and reliability. Reliability was a major factor because the attachment should ensure that the data collected is accurate and usable. With the use of SolidWorks, the attachment went through two iterations. The designs were 3D printed on the Ultimaker 3 and made of polylactide material. In Fig. 20 the first iteration is shown which was a bulkier design and did not have the ability to change angles easily. It also covered the whole ultrasound probe with no ability to produce any force on the probe towards the forearm. This attachment was meant to be aligned with the forearm. Through iterations, it helped the attachment be more fitting to the probe, also reducing the size, material required and overall cost to produce.

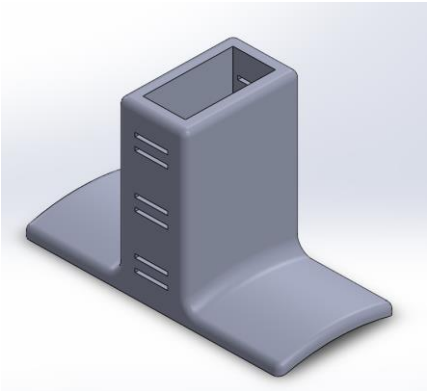

Figure 20: Probe Attachment Iteration 1

3.3.3 Collection Protocol

Adjacent work to this project was being pursued to develop machine learning algorithms to classify MCP joint angles from B-mode ultrasound images. Algorithms being tested included convolutional neural networks and recurrent neural networks. Data required for these algorithms to yield

success needed to be abundant, consistent, and varietal. It was determined that in order to meet these data requirements, collection would need to happen across ten subjects, performing eleven different hand motions, with two trials per motion. Appendix A outlines the testing protocol with the hand motions required for collection. During each collection period, 1400 frames of data could be collected and labelled. This would yield 308,000 data points to be trained on with a variety of movements. Consistency was acquired through the development of a probe attachment to fixate the ultrasound probe to the forearm.

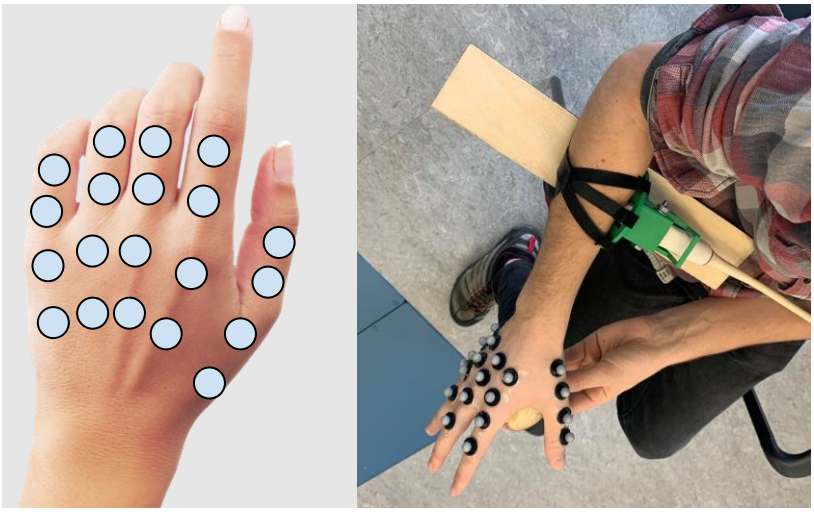

Figure 21: Marker Placement and Experiment Setup

3.3.4 Data Processing

Resulting from the data synchronization techniques used (detailed in section 3.3.1), data correlation was all done in post-processing. Following a single collection, several sets of data would be produced. These sets included a MATLAB data file (.mat) from the Verasonics ultrasound machine, a delimited text file (.csv) containing the Vicon motion capture data, and another delimited text file (.csv) containing the synchronization signal. It was known how many frames of data were contained in the ultrasound data file (1400 frames were used during our testing). Using this baseline, the synchronization file contained the data needed to correlate the ultrasound data with the motion capture data. For a single ultrasound frame, roughly 10-12 frames of motion capture data would exist. Using these excess frames, the average would be calculated and reduced to a single data point for a single frame of ultrasound data.

3.4 Prosthetic Motion & Software System Architecture Simulation

The purpose of the simulation is to provide a baseline model to develop the prosthetic from. It serves to allow for position control of fingers in one degree of freedom and testing of machine learning models in comparison to motion capture data. Using the metacarpophalangeal (MCP) joints as input, it will produce position outputs in space. These outputs are plotted using the 3D model.

To begin development of the simulation, design requirements were created. These requirements included: 1) ability to show independent finger movement in finger task space 2) convert MCP joint angles to task space 3) integrate with machine learning to convert ultrasound images into MCP joint angle predictions. Based on these design requirements, a couple of potential approaches were decided upon. These approaches served to combat uncertainty and provide alternative options in the case of failed pursuits, thus lowering the risk of complete failure. Chosen design approaches included the Asynchronous Multibody Framework (AMBF) and MATLAB.

3.4.1 Asynchronous Multibody Framework (AMBF)

The Asynchronous Multibody Framework was developed by a group of researchers at WPI. It allows for simulation of 3D models in real time as well as interaction with peripheral devices. Further, it integrates with Blender, an open-source 3D modeling software, to allow for simple generation of necessary dependencies in the AMBF. While this software appears ideal for our application, it lacked extensive documentation. This added uncertainty for our application.

3.4.2 MATLAB

MATLAB provides a simple pipeline for developing 3D plots in real time. This makes demonstration of position control relatively straightforward. While it does not support simulation of 3D models, plots can be created that resemble the proper movement of system components. MATLAB, being used in other aspects of system functionality makes integration of other MATLAB-based systems a relatively simple task. So, it was decided that the use of MATLAB would not yield the exact desired result, but it was determined to be a viable contingency plan.

3.4.3 Three.js

Three.js is a JavaScript library that uses WebGL for 3D computer graphics. Using this library would allow for the models used in the prosthetic designed to be manipulated in three-dimensional space inside of a web browser. Because it utilizes JavaScript, implementing that into a web-based platform is

relatively straightforward. Adjacent work has been pursued to host a web server for processing machine learning models and data. It has been developed such that images can be serialized and sent to the server and five predicted MCP joint angles will be produced in response. Using this library, a front-end platform can be integrated directly into that web server.

3.4.4 Simulation Approach

Based on the research done into the three different design approaches, it was determined that the AMBF would be pursued with a time block of two weeks given. If the time block time was exceeded and enough progress was not made, MATLAB would be pursued. Ultimately, after pursuing the use of the AMBF, MATLAB was used. The AMBF presented a number of implementation difficulties due to its limited documentation and overall use. Throughout this project, following the development of the MATLAB simulation, the Three.js approach was attempted to better integrate all systems.

3.5 Data Streaming

Preliminary simulation work and prosthetic development was done by cycling through saved data. This allowed development to proceed until real-time data streaming options existed. Real-time streaming of images was necessary in order to control the simulation and prosthetic in real time. Due to complexities with the Verasonics system, streaming data in real time was not as straightforward as it originally seemed. For this reason, multiple different approaches were attempted.

An approach using ROS was developed by a member of the Fusion Lab but was not originally pursued for implementation because of limitations in its throughput. The throughput was limited due to post-processing done on each frame of data. This caused only 8 frames per second to be possible. Ideally, 30 frames per second was possible. Approaches attempted were pursued in order to potentially increase this throughput to its maximum capabilities.

Desirable architecture was determined to remove as much external processing off of the Verasonics machine as possible. The central machine, running the machine learning server locally alongside the simulation and prosthetic control was then decided to be networked to the Verasonics machine. Data would then be serialized and sent over the network to the central machine. This architecture is further outlined below:

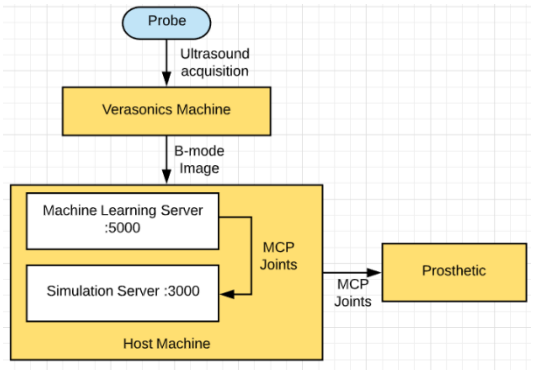

Figure 22: System Architecture Design

3.5.1 Approach 1 - Java Applet Modifications

Upon the start of a Verasonics script, the VSX viewer has access to the real-time images being captured. The VSX viewer is run as an external Java applet. Because of this, the first approach to access the real time images involved decompilation of the VSX viewer and externally injecting necessary code to stream the images to an external server. While this approach appeared promising, it was ultimately decided to abandon this approach when it was determined that the images accessed by the VSX viewer had post-processing applied to them. This was an issue because data collected for our machine learning algorithms did not have the post-processing applied to it.

3.5.2 Approach 2 - External Python Function Triggering

After consultation with experts on use of the Verasonics system, a viable approach was determined. This approach included the capability to trigger an external function written in python upon the capture of every frame. While this approach appears viable, it is not yet completed. More work needs to be done in the pursuit of this approach.

Chapter 4: Results

A complete probe orientation study was performed for this project. This study will influence the finalized design of the gauntlet of the hand prosthetic. While this is not incorporated in the results of the project, it presents a baseline for future work to be based. This uncertainty on probe orientation was known going into this project. Because of this, the focus of the prosthetic design was on the development of the components not directly influenced by this. Prior to the manufacturing of the prosthetic, a simulation was created in MATLAB to prove capabilities of machine learning. Due to extenuating circumstances removing access to campus, further work was pursued on the simulation. Ultimately a simulation was created in React and Three.js and demonstrates the kinematics of all components of the system.

4.1 Optimal Probe Orientation on Forearm

Different measures of accuracy were calculated to identify which probe orientation displays a higher magnitude of muscle change. For the consecutive image analysis, the data that was compared was made up of 60 frames which included 10 flexions of each motion. For the first image comparison the data used was the same as the one for consecutive image comparison, but this analysis was a derivative of the consecutive image analysis resulting in five flexions for each motion. The motion recorded as a reference was the hand at a stationary position. Having the motions compared to the reference, it can be seen that the cross-correlation values decrease, which is validated by the fact that that is where flexion occurred.

The quantified data revealed a statistically significant difference between the standard deviations of the two analyses. Fig. 23 displays the error graphs for both analyses comparing the 90° and 45° angle. In these graphs the error bars represent the standard deviations and the data points represent cross correlation averages. Standard deviations values are shown in Fig. 25, and Fig. 24 displays the cross-correlation averages. Since there is a higher error in the 90° compared to the 45° angle, it makes the 90° angle the optimal probe orientation. Having a greater error demonstrates more muscle movement.

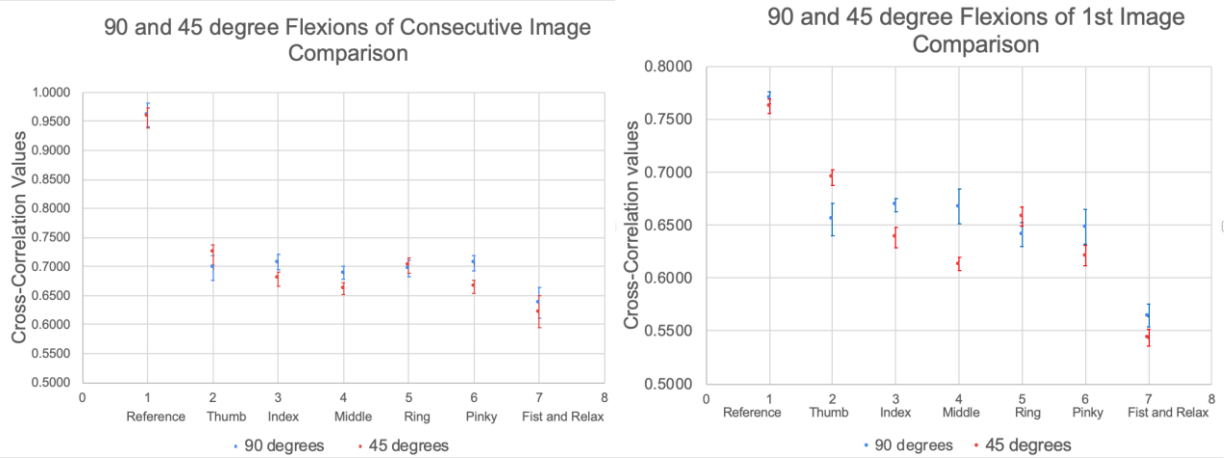

Figure 23: Error bar graphs of consecutive and first image comparison

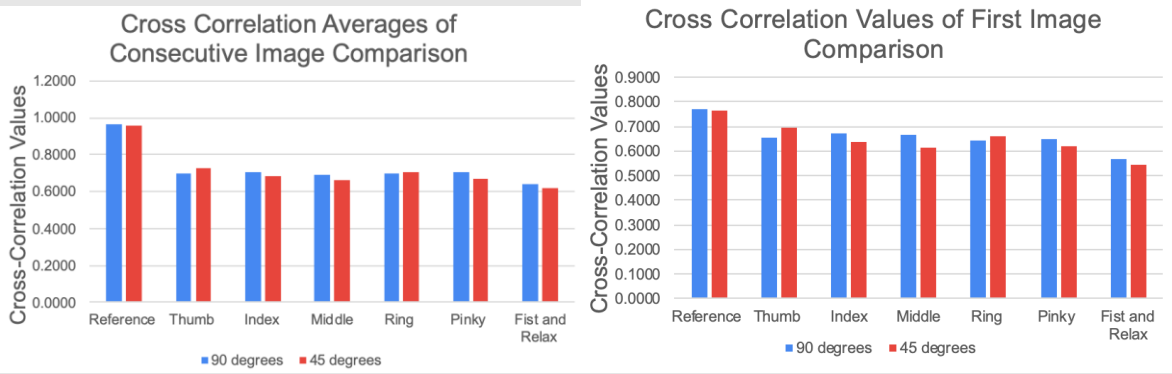

Figure 24: Cross correlation averages of each motion

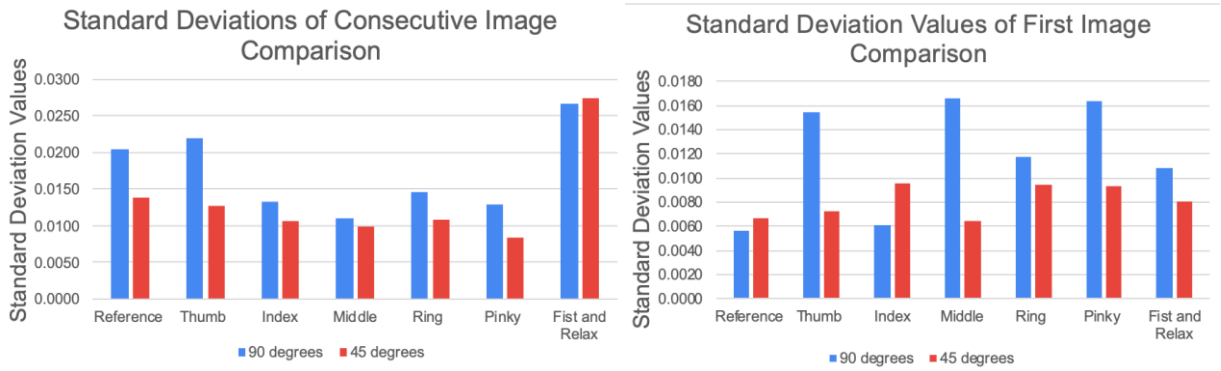

Figure 25: Standard deviation of each motion flexion

Previous analyses compared all motions, in this analysis we compared the right different regions of an ultrasound image. The graphs created each pertained to a motion tested, comparing the eight regions of the 90° angle to those of the 45° angle. A total of six error graphs were created with a corresponding histogram of standard deviations, Fig. 26 shows the results for the pinky image segmentation, all other graphs can be seen in Appendix B. For each error graph the cross correlation coefficients were plotted and the error bar displayed the standard deviations.

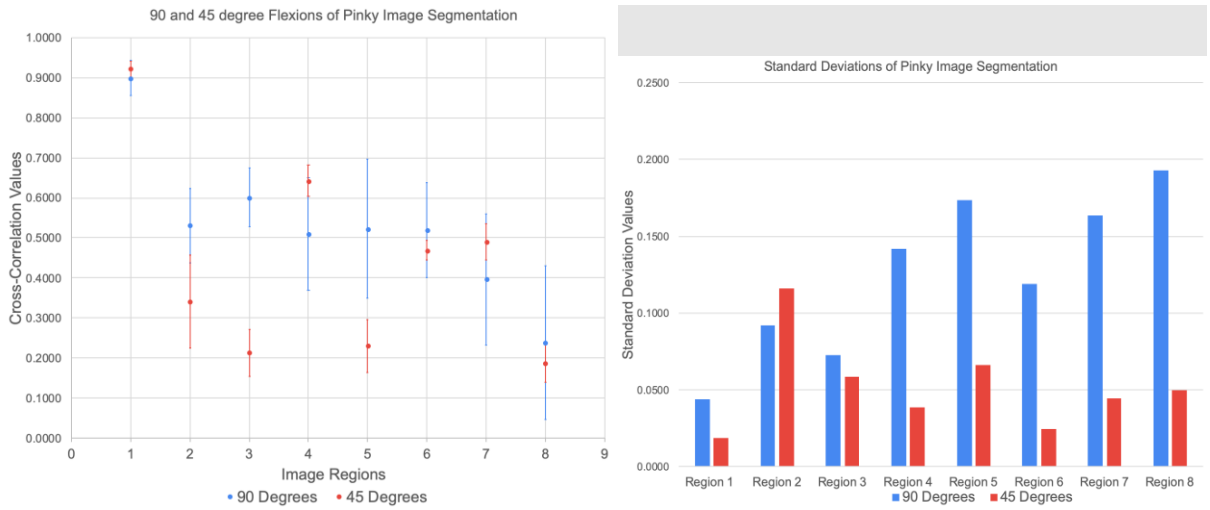

Figure 26: Error bar graphs of pinky flexions of image regions (on left) with the corresponding standard deviation histogram (on right)

Comparing subregions through cross correlation resulted in finding the optimal probe placement to continue being the 90° angle. Although there were regions in which the standard deviation was higher for the 45° angle. There was a constant higher value for the 90° angle comparing them to all the other motions. Graphs in Fig. 24 show how the cross-correlation values change overtime.

4.2 Design of Prosthetic

4.2.1 Prosthetic

From the finite element analysis' quantitative data were able to extrapolate the maximum stress experienced with each load amount. We found them to be .875MPa, 4.29MPa, 6.44MPa, and 8.58MPa for the 1N (SolidWorks simulation default), 500g, 1000g, and 1,500g loads respectively. When these values were compared to the material properties of soft PLA, which is the material utilized in the tested region, we found these values to be lower than the 16MPa yield strength. Our findings supported the original hypothesis. This is because the maximum probable stress due to loading is lower than the yield strength of the material being used in the highest loaded regions. From this information we have found that the prosthetic design will be able to support the potential loading it may experience when in use. Below is a table showing summary values of the data collected and highlighted are the maximum values from each sample segment.

Units (MPa)	**Hinge 1**				**Hinge 2**			
	Interior	**Exterior**	**Side 1**	**Side 2**	**Interior**	**Exterior**	**Side 1**	**Side 2**
MAX	8.36E+05	8.75E+05	8.75E+05	8.73E+05	2.77E+05	3.13E+05	3.12E+05	3.13E+05
MIN	3.93E+04	3.92E+04	7.82E+03	7.84E+03	7.78E+03	1.26E+04	2.81E+02	3.45E+02
Average	2.25E+05	2.37E+05	7.87E+04	7.91E+04	8.19E+04	9.36E+04	2.75E+04	2.75E+04

Table 2: 1N Surface Stress Values

Units (MPa)	**Hinge 1**				**Hinge 2**			
	Interior	**Exterior**	**Side 1**	**Side 2**	**Interior**	**Exterior**	**Side 1**	**Side 2**
MAX	4.10E+06	4.29E+06	4.29E+06	4.28E+06	1.36E+06	1.53E+06	1.53E+06	1.53E+06
MIN	1.93E+05	1.92E+05	3.84E+04	3.84E+04	3.81E+04	6.17E+04	1.38E+03	1.69E+03
Average	1.10E+06	1.16E+06	3.86E+05	3.88E+05	4.01E+05	4.59E+05	1.35E+05	1.35E+05

Table 3: 500g Surface Stress Values

Units (MPa)	**Hinge 1**				**Hinge 2**			
	Interior	**Exterior**	**Side 1**	**Side 2**	**Interior**	**Exterior**	**Side 1**	**Side 2**
MAX	6.15E+06	6.44E+06	6.44E+06	6.42E+06	2.04E+06	2.30E+06	2.30E+06	2.30E+06
MIN	2.89E+05	2.88E+05	5.75E+04	5.77E+04	5.72E+04	9.26E+04	2.07E+03	2.54E+03
Average	1.66E+06	1.74E+06	5.79E+05	5.82E+05	6.02E+05	6.88E+05	2.02E+05	2.02E+05

Table 4: 1000g Surface Stress Values

Units (MPa)	**Hinge 1**				**Hinge 2**			
	Interior	**Exterior**	**Side 1**	**Side 2**	**Interior**	**Exterior**	**Side 1**	**Side 2**
MAX	8.20E+06	8.58E+06	8.58E+06	8.56E+06	2.71E+06	3.07E+06	3.06E+06	3.07E+06
MIN	3.85E+05	3.84E+05	7.67E+04	7.69E+04	7.63E+04	1.23E+05	2.75E+03	3.38E+03
Average	2.21E+06	2.32E+06	7.72E+05	7.76E+05	8.03E+05	9.18E+05	2.69E+05	2.69E+05

Table 5: 1500g Surface Stress Values

Referencing the data above, the maximum value is 8.58 MPa which is still far below the yield strength of the material.

4.2.2 Gauntlet

Several iterations of the prosthetic gauntlet were produced based on the identified requirements. Each design was made to address items from the list of specifications we created. The final design we came to is below, shown in Fig. 27. This design addressed all the requirements discussed in section 3.2.4 and supported the freedom to rotate the motors in different orientations as to optimize the space available on the platform.

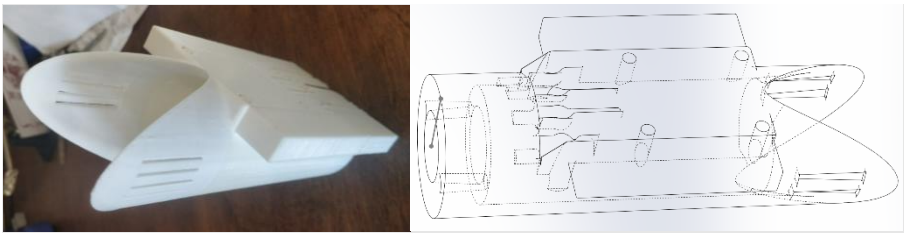

Figure 27: Prosthetic Gauntlet

4.3 Data Acquisition

4.3.1 Collection & Machine Learning

Only one subject's quantity of data across one trial per motion was able to be collected. Due to complexities in system synchronization, limited access to the Vicon and Verasonics machines, as well as sheer collection time, the quantity of data desired was not met. Each set of data, 1400 frames in length, took 30 seconds to acquire. However, data processing and transfer to an external drive took upwards of 15

minutes per data acquisition. Applying the data acquired to a convolutional neural network did not yield results desired. Fig. 28 shows some of these preliminary findings. Further work to improve this data and the predictions was done in an adjacent project. However, due to extenuating circumstances relating to campus presence, more data was not capable of being collected.

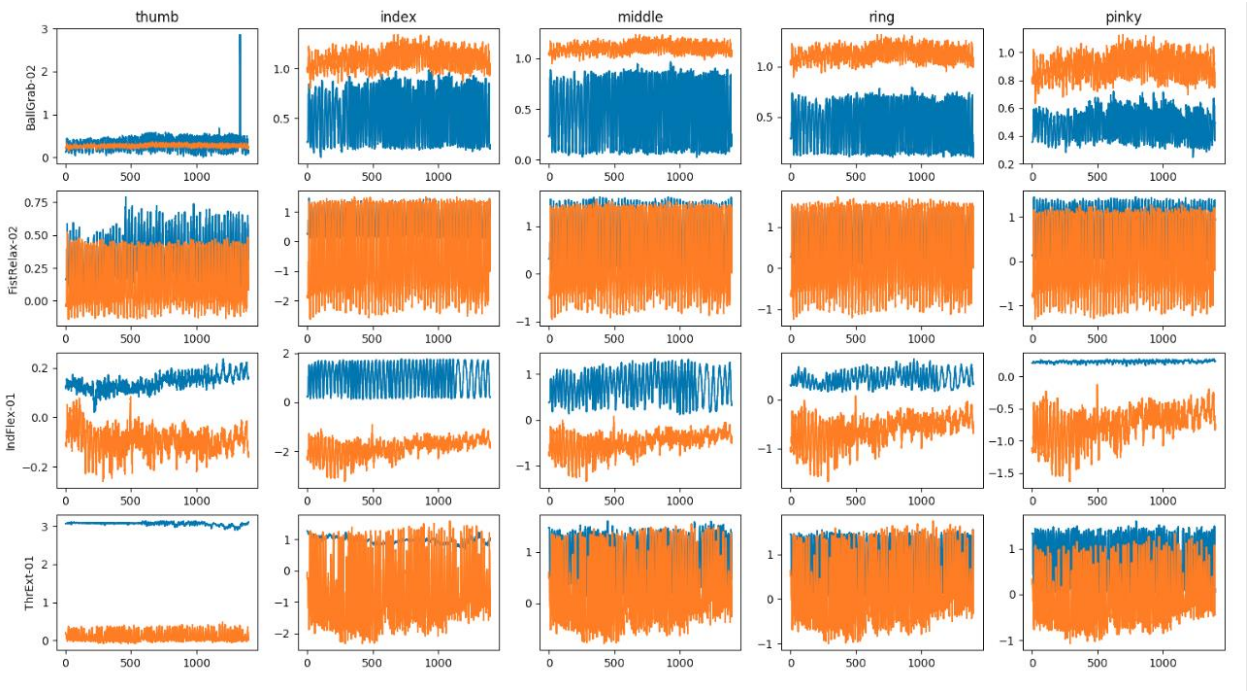

Figure 28: CNN Preliminary Data

Data representing each finger across four different datasets used for training and testing. These correspond to motions found in Appendix A.

(Predicted-Orange, Actual-Blue) (x: frames, y: radians of flexion)

4.3.2 Probe Attachment

The final iteration was the one used for testing; this is shown in Fig. 30. This iteration has a 4-inch diameter base and the whole design has a height of 5 inches. This attachment also consists of cuts on the base in which Velcro will be inserted to attach it to the forearm. There are 1inch cuts in the circumference of the base that are at 45° angles from each other, making it easy to change from 90° angle to a 45° angle. Two holes located on both sides of the design allow a bolt to pass through. The bolt would align with the curved section of the probe, working as a support to keep the probe inside the attachment and providing a constant force on the forearm. This probe configuration allowed for the subject to have their forearm in a neutral position or supinated 90°. The top rectangular section of the attachment was used as a stand to keep the probe stable onto the surface.

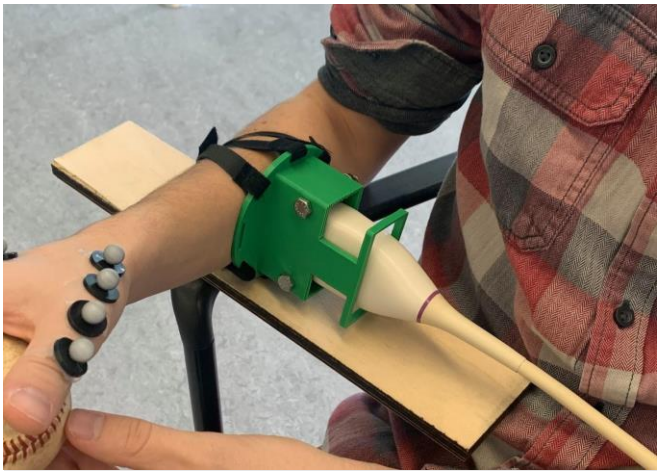

Figure 29: Ultrasound Data Collection Setup

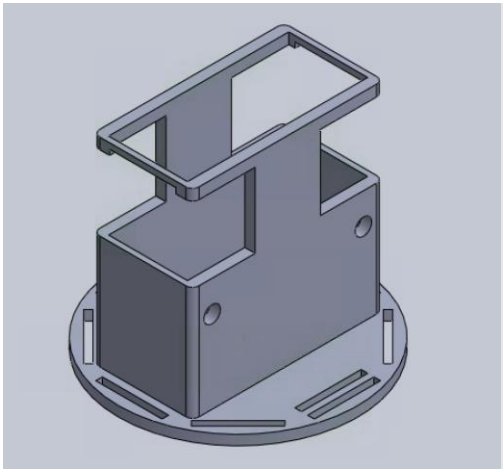

Figure 30: Ultrasound Probe Support Device

4.4 Prosthetic Motion & Software Systems Architecture Simulation

4.4.1 MATLAB

The data processing pipeline begins with data collection on the Verasonics machine. For post-processing use, this data is saved and packaged up in a cell array containing all ultrasound information. Such data includes RF-data and B-mode images. Using the B-mode images, from previously collected datasets, machine learning models were trained and developed by another MQP project. A RESTful API was created by that project that would allow an image to be passed to it via a POST request to the web server that it ran on. This web server would reply with predicted MCP joint angles based on that machine learning model.

MCP joint angles would then be used to calculate the forward kinematics of the following linkages in the finger. So, positions for the proximal interphalangeal (PIP), distal interphalangeal joints

(DIP), and the fingertip were calculated by identifying the DH-parameters of the fingers and using the resulting transformation matrices. Using the MCP joint angles, an assumption was made regarding the trajectory of the downstream joints that the PIP joint would match the angle of the MCP joint, and the DIP would remain at a constant 10° flexion. While this assumption does not exactly hold true to reality,

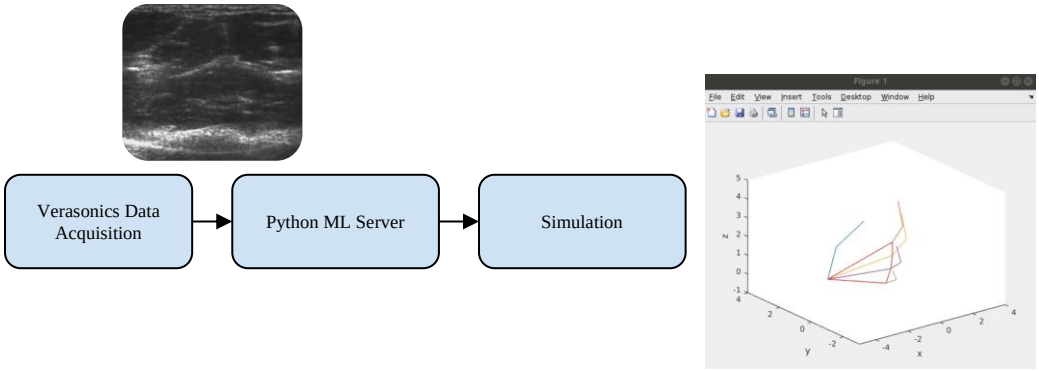

Figure 31: Simulation Process Map

limitations of the machine learning model do exist in that it is only capable of predicting the MCP joint angles and not all joint angles of the finger. Further, data for thumb support does not exist in the data sets that the machine learning models have been trained for. Because of this, the simulation does not support thumb movement with integration into the machine learning pipeline. However, it does support movement across one degree of freedom.

4.4.2 Three.js & React

In the final revision of the simulation, the entire architecture was redesigned such that it controlled the actual hand we designed based on ultrasound input. This was created using a JavaScript framework, React, as a container and Three.js to handle the three-dimensional animation. When objects are loaded into the scene in Three.js, manipulation of them presented some unique challenges. Each object is offered six degrees of freedom: (x, y, z) placement and (x, y, z) rotation. Operations to perform their manipulation are done in the respective order. Like the MATLAB approach, each of the base positions was calculated using DH-parameters and creating respective transformation matrices. Using these matrices, the rotation of elements was able to be extracted and applied to the initial offset about the x-axis for each element. For

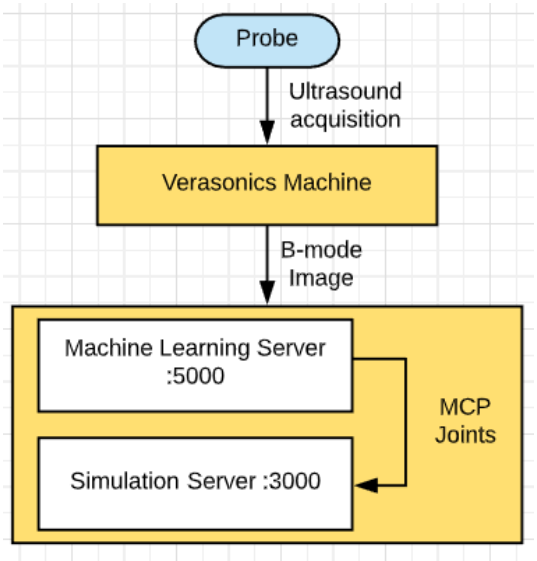

Figure 32: Data Processing Map

the simulation to receive the MCP joint angles, a new API was implemented into the existing machine learning server that would allow for images to be supplied and for the joint angles to be read. Because the data is being generated from a MATLAB data file (.mat), MATLAB was still producing the image being used. This image was serialized and sent to the newly developed restful POST endpoint `/api/supplyImage`. When a new image was supplied, processing would be done, and the new angles would be put into a json format and published to `/api/getAngle`. This simulation polls this API endpoint, processes angles published on it, and moves the hand to the respective joint angles.

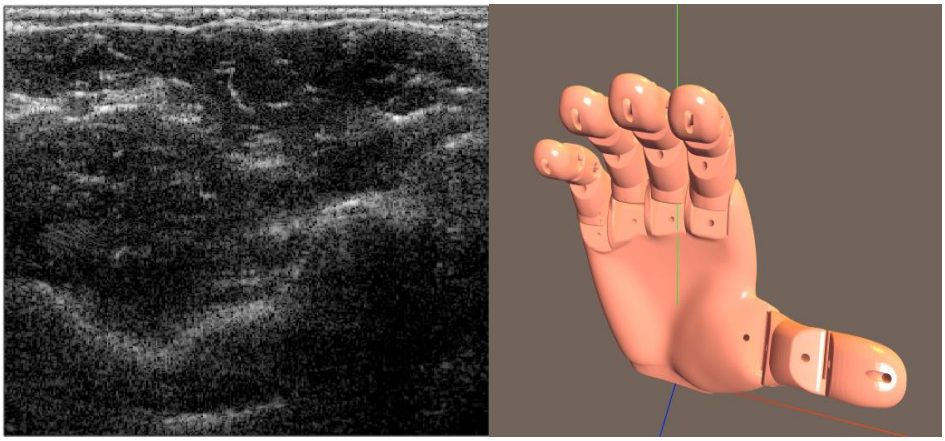

Figure 33: Ultrasound Image Correlation

Chapter 5: Discussion

5.1 Optimal Probe Orientation

5.1.1 Consecutive and First Image Analyses

Data from the present study indicates that the 90° angle is shown to perform the best. Allowing for a more precise recognition of muscle movement. This shows that a wider range of muscles are viewed with the probe at this orientation. Standard deviations were significantly different not just between different angles but also between different motions. Fig. 25 (shown in section 4.1), it is seen that the standard deviations for the consecutive comparisons were similar between angles, at first this resulted in both orientations being precise. Although in the first image comparison the standard deviations vary between angles and positions. These results showed a greater standard deviation value for the 90° angle. Even though it can be seen that there is a difference in the index flexion, displaying that the standard deviation is higher for the 45° angle, this could have been a result of how the data was collected. An improvement that can be made is having more repetitions of data collection at both angles to see if the results align and allowing for more accurate results.

Even though standard deviations may vary the 90° angle was shown to have higher values, showing a greater error. One possible reason for this is that placing the probe at a 90° angle has a good coverage of the tendons. The tendons that move the fingers are more precisely covered by this probe orientation. Allowing for the ultrasound images to display images that allow for the visualization of the muscles from different finger movements.

5.1.2 Image Segmentation Analyses

The intention of this analysis was to study the change of muscle happening at the specific regions of the images. The results of the study hereby reported clearly show that the 90° angle is optimal. The team applied the algorithm which was able to segment images of different motions and quantify it. This allowed for a closer analysis of the data set collected. There were six motions that were analyzed, and each was divided into eight regions resulting in 48 different standard deviations. Out of the 48 standard deviations 17 of them were greater for the 45° angle and 31 of them for the 90° angle. The results show that the average of error was 65 % greater in the 90° angle than in the 45° angle. The 45° angle was statistically shown to have less error, meaning there is a limited range of muscle movement that is viewed by the ultrasound probe. More error shown pertains to change of muscle magnitude. The trend observed

between the two angles was that the correlation coefficients were close in range per region of each hand motion. This means that muscles had a similar magnitude change per region. Standard deviations decreased going from the 90-degree angle to the 45-degree angle, showing that more motion movement was present in the 90-degree angle. The only standard deviations that were similar were the fist and relax since all fingers were moving simultaneously.

Cross-correlations obtained are lower than that of the reference point because it shows that there was movement in the muscles. But not all cross-correlations per region were the same value, values varied depending on the region and the conditions that were tested. This result is because the regions compared were the same, meaning 90° thumb flexion region 1 was compared to 45° thumb flexion region 1. Even though the same regions were compared there was a difference in values, this could be due to the accuracy in each flexion. The test subject could have extended its fingers at slightly different angles each time. It could also be due to probe manipulation. Manipulating the probe results in differences in ultrasound images. When testing with the ultrasound probe maneuvers such as pressure, alignment, rotation and tilt are important. Tilt, rotation and alignment were all factors that were considered when the probe attachment was made. Those factors were constant throughout data collection. The variation in results could be due to pressure and ultrasound gel. Pressure from the test subject on the probe could have affected the images being produced. It is also to be noted that during the seven different motions there was no addition of ultrasound gel so that we did not have to remove the probe from its location. The results show that the muscle magnitude affects each region differently, with 90° being the position in which the probe should be placed on the prosthetic.

In summary, the results suggest that there is a greater error in the 90° angle probe orientation in showing magnitude in muscle change. This orientation is superior to the 45° angle.

5.2 Prosthetic

Although the gauntlet and prosthetic design were enough for our desired application, they can certainly still be improved upon in the future to better meet consumer needs. From the research and weighted matrix created, we identified a list of priorities for the prosthetic. Not all of these were addressed but would certainly be ideal in a final product. The reasoning for some of these not being in our product varied from time constraints to mechanical. One of the recommended improvements is the joining of the last to finger joints as it reduces the chance of part failure. Another is the use of nylon and more specifically skin tone materials as consumers reported that they value a prosthetic that is visually similar to a normal hand. This customization option would be valued. With regards to the gauntlet, moving all components internally would be ideal as to not only protect it, but also make it more visually appealing.

One difficulty in doing this is the space available inside the forearm. There is not a large amount available so a strong base in robotics and electrical wiring would be recommended to undertake this.

5.3 Simulation

While this simulation is a good starting point for a prosthetic to be constructed, there exist some limitations and areas for improvement. Processing of an ultrasound image takes quite a long time. Currently, one image takes upwards of three seconds to process. With a collection frequency of 25 Hz, this is far too inefficient to display movement in real time. More experimentation needs to be done to decide on the costly aspects of this computation. A preliminary review of this indicates that some of the processing time is caused by a large amount of processes on the host machine. Because the machine learning web server is running locally in addition to MATLAB loading several gigabytes of saved ultrasound data, many computer resources are used. Additionally, images are being cycled through fairly quickly. Experimentation needs to be done to determine the optimal sampling rate of the ultrasound data regarding movement of the prosthetic and the simulation.

Chapter 6: Conclusion

With the conclusion of our work on this project, we have been able to accomplish many of the goals we set in the beginning. One such goal was to produce a viable prosthetic. Another was the production of a way to present our project visually and test it virtually which we accomplished with a simulation. Lastly, we conducted a study on the optimal probe orientation which concluded that 90 degrees is optimal for data collection and translation. To help this project continue to succeed we have also built a framework with our recommendations for the future to ensure that this project continues to develop and grow. With these outcomes we were able to continue the process of empowering prosthetic users with the use of ultrasound sensing technology.

Chapter 7: Recommendations

Throughout this project, a few problems were encountered that either rendered some of the approaches used as ineffective or resulted in non-optimal systems designed. A few areas that could be improved upon for future work to build off of include prosthetic design choices and use of the Verasonics ultrasound machine.

Our first recommendation would be to combine the medial and distal phalanx on the prosthetic. Neither of these links are actively actuated. Because of this, they are susceptible to position control error. If these two links are combined, tactile feedback would be improved, and it would still meet the design requirements of the hand. Another recommendation regarding the prosthetic design would be to develop a protocol to test outcomes of the prosthetic. Using this protocol, work backwards to make design choices that make sense for the specific outcomes desired. Throughout this project, one issue that we constantly worked through from a design perspective was trying to operate on too broad of requirements. If the requirements were constrained, it is likely that it would have resulted in a more complete hand design.

From a software perspective, we have a couple of additional recommendations. First, learn how to use the Verasonics machine. By the end of the project, we eventually learned how to use it in the capacity that was required. However, using this machine presented many issues throughout the entire duration of this project. If more upfront time had been spent learning how to use this machine and the varying capabilities of it, many issues encountered with data streaming and synchronization would have been much quicker to debug.

Our last recommendation would be to get data streaming working. Data streaming refers to the transfer of ultrasound data in real time to anywhere that is not the Verasonics machine. This is necessary for a few reasons. First, eventually the prosthetic will need to support real time processing. Second, transferring data from the Verasonics machine following a data collection can take upwards of 10-20 minutes. Resulting from this, data collection took a substantial amount of time for small quantities of data.

References

Ackerman, Evan. "'Skywalker' Prosthetic Hand Uses Ultrasound for Finger-Level Control." *IEEE Spectrum: Technology, Engineering, and Science News*, 12 Dec. 2017, spectrum.ieee.org/the-human-os/biomedical/devices/skywalker-prosthetic-hand-uses-ultrasound-sensors-for-fingerlevel-control.

Cabibihan, J.-J., Joshi, D., Srinivasa, Y., Chan, M. A., & Muruganantham, A. (2014). Illusory Sense of Human Touch from a Warm and Soft Artificial Hand. *IEEE Transactions on Neural Systems and Rehabilitation Engineering*, 1–1. doi: 10.1109/tnsre.2014.2360533

Castellini, C., and Passig, G. Ultrasound image features of the wrist are linearly related to finger positions. In *Intelligent Robots and Systems (IROS), 2011 IEEE/RSJ International Conference on*, IEEE (2011)

Chen, Xin, et al. "Sonomyography (SMG) Control for Powered Prosthetic Hand: A Study with Normal Subjects." *Ultrasound in Medicine & Biology*, vol. 36, no. 7, 2010, pp. 1076–1088., doi:10.1016/j.ultrasmedbio.2010.04.015.

Densford, Fink. "Researchers Create Ultrasound-Sensor Powered Prosthetic Hand with Individual Digit Control." *The Robot Report*, 12 Dec. 2017, www.therobotreport.com/researchers-create-ultrasound-sensor-powered-prosthetic-hand-individual-digit-control/.

Douglas, Tania, et al. "Ultrasound Imaging in Lower Limb Prosthetics." *IEEE Transactions on Neural Systems and Rehabilitation Engineering : a Publication of the IEEE Engineering in Medicine and Biology Society*, U.S. National Library of Medicine, Mar. 2002, www.ncbi.nlm.nih.gov/pubmed/12173735.

"Electromyography (EMG)." *Electromyography (EMG) | Johns Hopkins Medicine*, www.hopkinsmedicine.org/health/treatment-tests-and-therapies/electromyography-emg.

Filament2Print. 2020. 20 April 2020. <https://filament2print.com/gb/special-pla/660-soft-pla-flex.html>.

"Flexor and Extensor Tendon Laceration." *Midwest Orthopedics at Rush*, www.rushortho.com/body-part/hand/flexor-extensor-tendon-laceration.

Guo, Jing-Yi, et al. "Dynamic Monitoring of Forearm Muscles Using One-Dimensional Sonomyography System." *Journal of Rehabilitation Research and Development*, U.S. National Library of Medicine, 2008, www.ncbi.nlm.nih.gov/pubmed/18566937.

"Human Hand Anatomy Anterior View Diagram." *Anatomy Note*, 30 Sept. 2018, www.anatomynote.com/human-anatomy/extremity-anatomy/human-hand-anatomy-anterior-view-diagram/.

Huinink, L., et al. “Learning to use a body-powered prosthesis: changes in functionality and kinematics.” (2016). *Journal of neuroengineering and rehabilitation*, *13*(1), 90. https://doi.org/10.1186/s12984-016-0197-7

Jones, Oliver. “Muscles of the Hand.” *TeachMeAnatomy*, 10 May 2018, teachmeanatomy.info/upper-limb/muscles/hand/.

Karlık, Bekir. “Machine Learning Algorithms for Characterization of EMG Signals.” International Journal of Information and Electronics Engineering, vol. 4, no. 3, May 2014, doi:10.7763/ijiee.2014.v4.433.

Kazamel, Mohamed, and Paula Province Warren. *History of Electromyography and Nerve Conduction Studies: A Tribute to the Founding Fathers*. 43 Vol. , 2017. Web.

Kim, Jeong Ho, and Peter W. Johnson. “Viability of Using Digital Signals from the Keyboard to Capture Typing Force Exposures.” *Ergonomics*, vol. 55, no. 11, 17 Aug. 2012, pp. 1395–1403., doi:10.1080/00140139.2012.709542.

Loricchio, David F. “Key Force and Typing Performance.” *Proceedings of the Human Factors Society Annual Meeting*, vol. 36, no. 4, 1992, pp. 281–282., doi:10.1177/154193129203600404.

Koundal, Deepika, and Bhisham Sharma. “Advanced Neutrosophic Set-Based Ultrasound Image Analysis.” *Neutrosophic Set in Medical Image Analysis*, Academic Press, 1 Nov. 2019, www.sciencedirect.com/science/article/pii/B9780128181485000035.

Kuentz, Lily, et al. “Additive Manufacturing and Characterization of Polylactic Acid (PLA) Composites Containing Metal Reinforcements.” *NASA*, NASA, 2016, ntrs.nasa.gov/search.jsp?R=20160010284.

Makerbot Thingverse: Dextrus Hand. 2 April 2014. 1 December 2019.

Makerbot Thingverse: Odysseus Hand. 4 March 2014. 1 December 2019.

Makerbot Thingverse: Osprey Hand. 4 July 2015. 1 December 2019.

Makerbot Thingverse: Phoenix Hand. 30 March 2016. 1 December 2019.

Makerbot Thingverse: Raptor Hand. 17 December 2014. 1 December 2019.

Makerbot Thingverse: Talon Hand. 19 January 2014. 1 December 2019.

MatterHackers. 2020. 20 April 2020. <https://www.matterhackers.com/store/l/175mm-blue-soft-pla-threequarter-kg/sk/M8JHED58>.

Moores, Danielle, and Erica Cirino. “Electromyography (EMG).” *Healthline*, Healthline Media, 20 Mar. 2018, www.healthline.com/health/electromyography.

N. Akhlaghi et al., "Real-Time Classification of Hand Motions Using Ultrasound Imaging of Forearm Muscles," in *IEEE Transactions on Biomedical Engineering*, vol. 63, no. 8, pp. 1687-1698, Aug. 2016, doi: 10.1109/TBME.2015.2498124

NIH 3D Print Exchange: K-1 Hand. 29 July 2015. 1 December 2019.

“Ottobock North America Consumer Home: Ottobock US.” Ottobock, www.ottobockus.com/.

Plagenhoef, Stanley, et al. “Anatomical Data for Analyzing Human Motion.” *Research Quarterly for Exercise and Sport*, vol. 54, no. 2, 1983, pp. 169–178., doi:10.1080/02701367.1983.10605290.

Pololu Metal Gearmotor 1000:1 *Micro Metal Gearmotor*. n.d. 22 April 2020. <https://www.pololu.com/product/3057>.

“Prostheses - Prosthetics: Artificial Limb Information.” Disabled World, Disabled World, 18 Mar. 2019. Web

Rafiee, J., et al. “Feature Extraction of Forearm EMG Signals for Prosthetics.” *Expert Systems with Applications*, vol. 38, no. 4, 2011, pp. 4058–4067., doi:10.1016/j.eswa.2010.09.068.

Rau, G, et al. “From Cell to Movement: to What Answers Does EMG Really Contribute?” *Journal of Electromyography and Kinesiology : Official Journal of the International Society of Electrophysiological Kinesiology*, U.S. National Library of Medicine, Oct. 2004, Web

"SD3D." 2020. SD3D. 20 April 2020. <https://www.sd3d.com/wp-content/uploads/2017/06/MaterialTDS-PLA_01.pdf>.

Sikdar, Siddhartha, et al. “Novel Method for Predicting Dexterous Individual Finger Movements by Imaging Muscle Activity Using a Wearable Ultrasonic System.” *IEEE Transactions on Neural Systems and Rehabilitation Engineering : a Publication of the IEEE Engineering in Medicine and Biology Society*, U.S. National Library of Medicine, Jan. 2014, www.ncbi.nlm.nih.gov/pubmed/23996580.

Stock, Matt S., et al. “Effects of Fatigue on Motor Unit Firing Rate versus Recruitment Threshold Relationships.” Muscle & Nerve, vol. 45, no. 1, 2011, pp. 100–109., doi:10.1002/mus.22266.

Sudarsan, S., and E. Chandra Sekaran. “Design and Development of EMG Controlled Prosthetics Limb.” *Procedia Engineering*, vol. 38, 2012, pp. 3547–3551., doi:10.1016/j.proeng.2012.06.409.

Taylor, Craig L., and Robert J. Schwarz. “The anatomy and mechanics of the human hand.” *National Academy of sciences-National Research Council*, May 1995. Web.

T. W. S. Kwong. *The 2015 IEEE International Conference on Systems, Man, and Cybernetics [Conference Reports]*. 2 Vol. , 2016. Web.

Jr, William C. Shiel. “Definition of Bones of the Arm, Wrist and Hand.” *MedicineNet*, 27 Dec. 2018, Web.

Ventimiglia, Paul. “Design of a Human Hand Prosthesis.” *Wpi.edu, Worcester Polytechnic Institute*, 26 Apr. 2012, Web.

Wood, Steve. 2014. “FlexyHand 2.” 3 July 2014, https://www.thingiverse.com/thing:380665.Accessed November 19, 2019.

Xie, Hong-Bo, et al. “Estimation of Wrist Angle from Sonomyography Using Support Vector Machine and Artificial Neural Network Models.” *Medical Engineering & Physics*, vol. 31, no. 3, 2009, pp. 384–391., doi:10.1016/j.medengphy.2008.05.005.

Zarzycka N., Załuska S. [Measurements of the arm in inhabitants of the Lublin region]. 1989. Web. 22 April 2020.

Zuniga, Jorge. *Makerbot Thingverse: Cyborg Beast*. 2 March 2014. 1 December 2020.

Appendices

Appendix A: Collection Protocol

Motion: Fist & Relax
Trials: 2
Explanation: Subject's hand begins in a relaxed open state, then closes. This process is repeated for the entire collection period.
Demonstration:

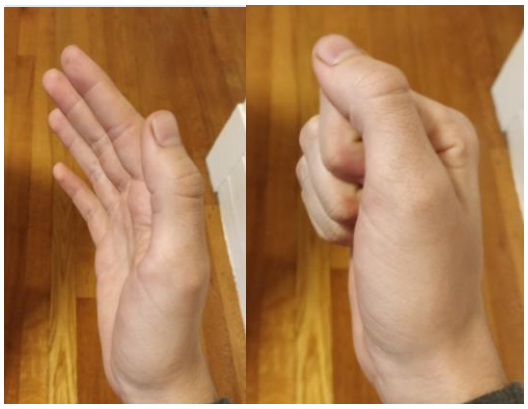

Motion: Bottle Grab
Trials: 2
Explanation: Subject's hand begins in a relaxed open state, then closes hand around a cylindrical bottle. This process is repeated for the entire collection period.
Demonstration:

Motion: Baseball Grab
Trials: 2
Explanation: Subject's hand begins in a relaxed open state, then closes hand around a baseball. This process is repeated for the entire collection period.
Demonstration:

Motion: Thumb Flexion
Trials: 2
Explanation: Subject's hand begins in a relaxed open state, then closes only the thumb. This process is repeated for the entire collection period.
Demonstration:

Motion: Index Flexion
Trials: 2
Explanation: Subject's hand begins in a relaxed open state, then closes only the index finger. This process is repeated for the entire collection period.
Demonstration:

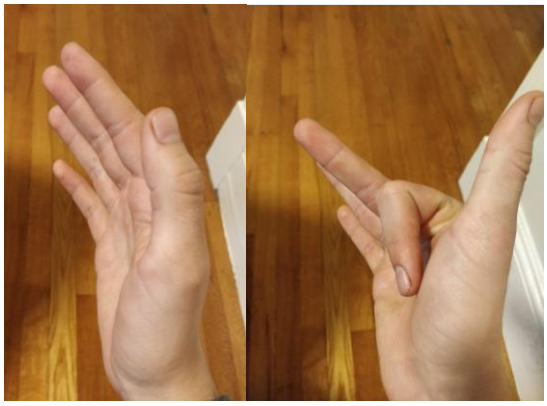

Motion: Middle Flexion
Trials: 2
Explanation: Subject's hand begins in a relaxed open state, then closes only the middle finger. This process is repeated for the entire collection period.
Demonstration:

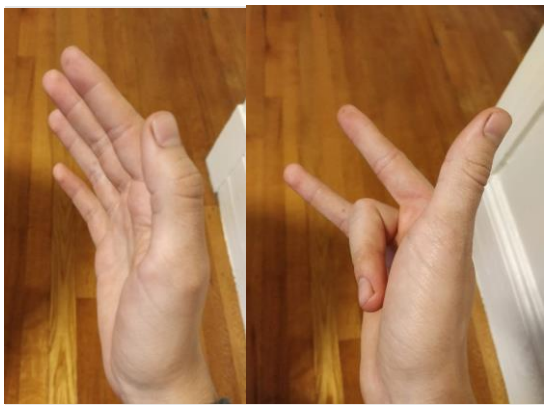

Motion: Ring Flexion
Trials: 2
Explanation: Subject's hand begins in a relaxed open state, then closes only the ring finger. This process is repeated for the entire collection period.
Demonstration:

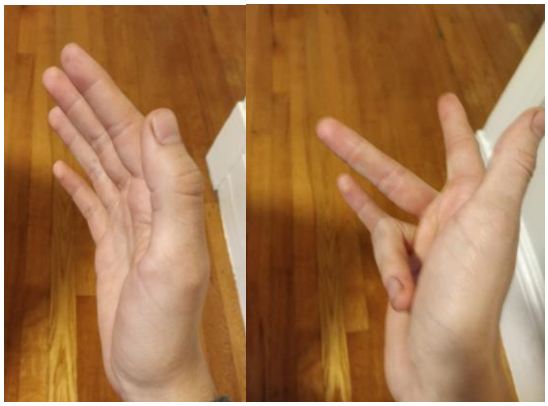

Motion: Pinky Flexion
Trials: 2
Explanation: Subject's hand begins in a relaxed open state, then closes only the pinky. This process is repeated for the entire collection period.
Demonstration:

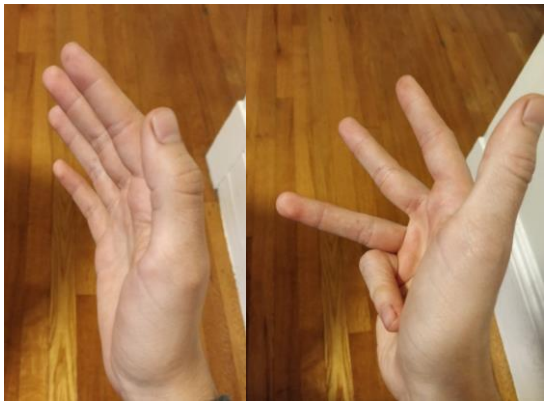

Motion: Thumb Extension
Trials: 2
Explanation: Subject's hand begins in a relaxed closed state, then extends only the thumb to an open state. This process is repeated for the entire collection period.

Demonstration:

Motion: Index Extension

Trials: 2

Explanation: Subject's hand begins in a relaxed closed state, then extends only the index finger to an open state. This process is repeated for the entire collection period.

Demonstration:

Motion: Middle, Ring, Pinky Extension

Trials: 2

Explanation: Subject's hand begins in a relaxed closed state, then extends only the middle, ring, and pinky fingers to an open state. This process is repeated for the entire collection period.

Demonstration:

Appendix B: Image Segmentation

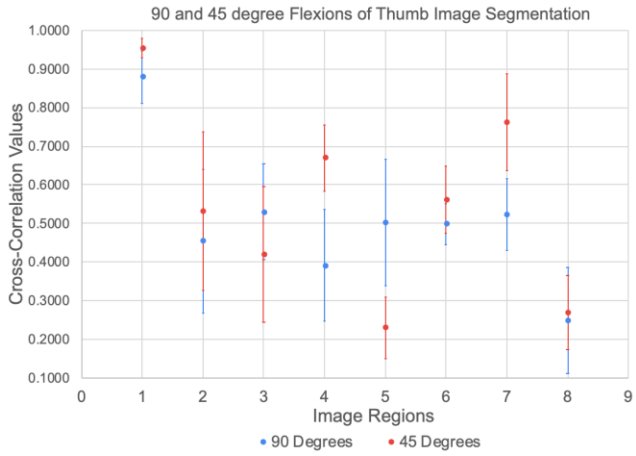

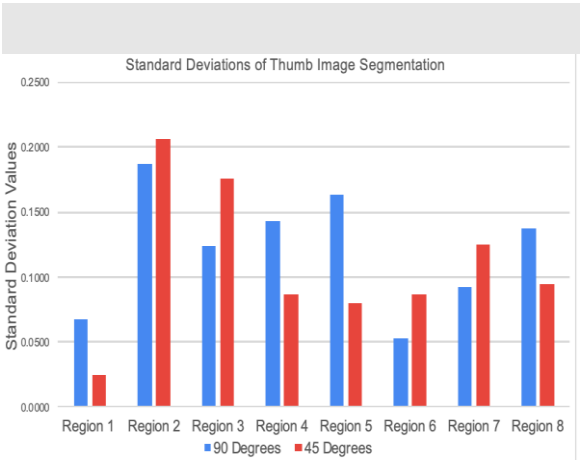

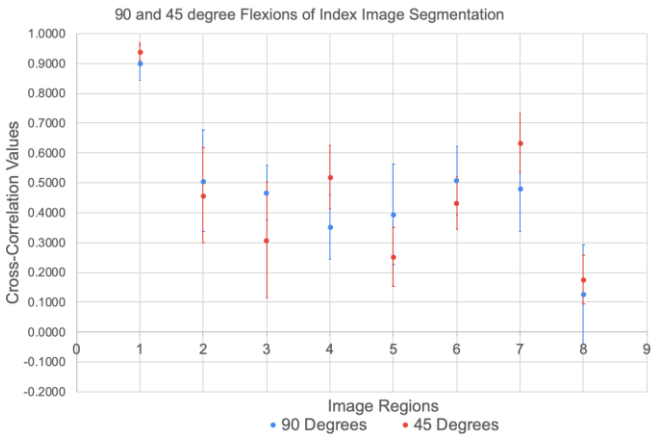

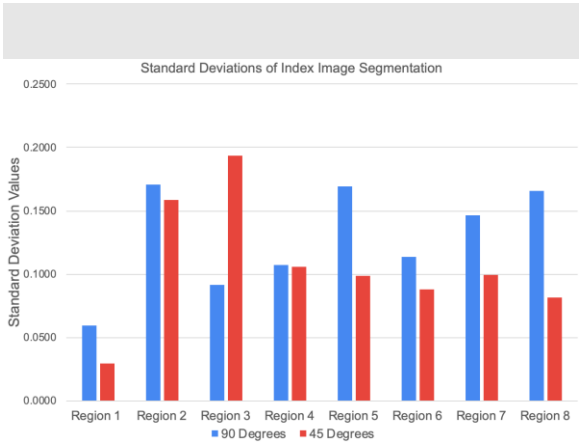

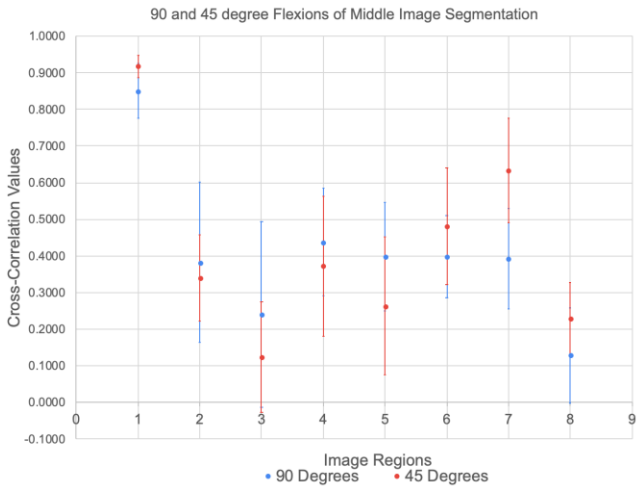

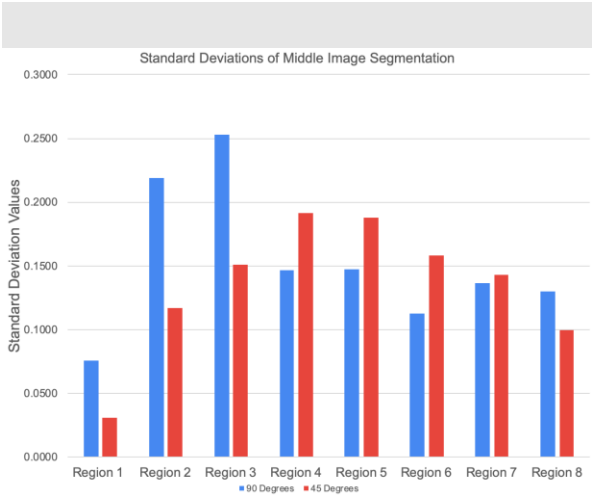

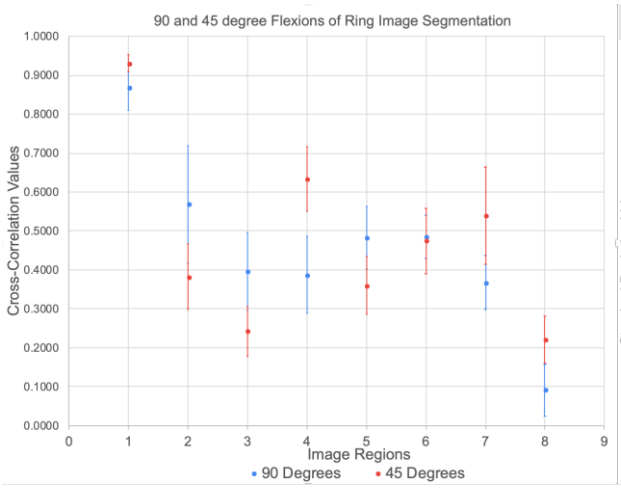
90 and 45 degree Flexions of Ring Image Segmentation
Cross-Correlation Values
Image Regions
90 Degrees
45 Degrees

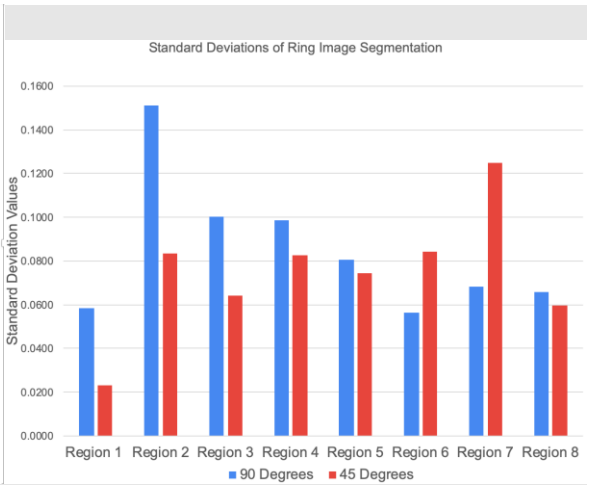
Standard Deviations of Ring Image Segmentation
Standard Deviation Values
Region 1
Region 2
Region 3
Region 4
Region 5
Region 6
Region 7
Region 8
90 Degrees
45 Degrees

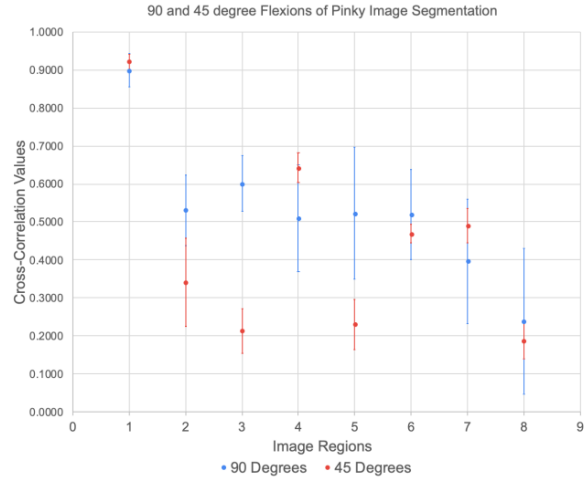
90 and 45 degree Flexions of Pinky Image Segmentation
Cross-Correlation Values
Image Regions
90 Degrees
45 Degrees

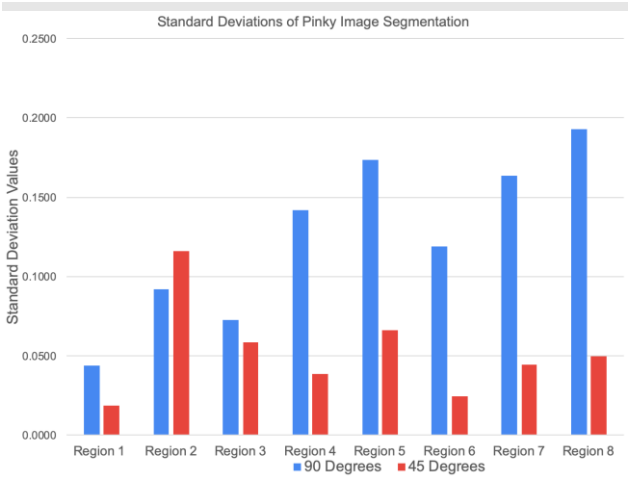
Standard Deviations of Pinky Image Segmentation
Standard Deviation Values
Region 1
Region 2
Region 3
Region 4
Region 5
Region 6
Region 7
Region 8
90 Degrees
45 Degrees

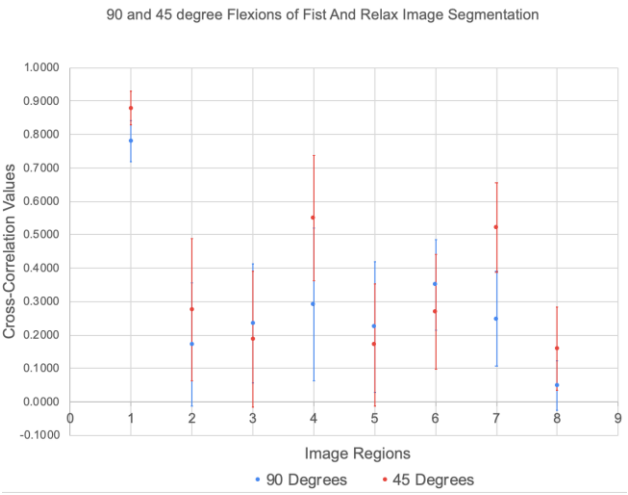
90 and 45 degree Flexions of Fist And Relax Image Segmentation
Cross-Correlation Values
Image Regions
90 Degrees
45 Degrees

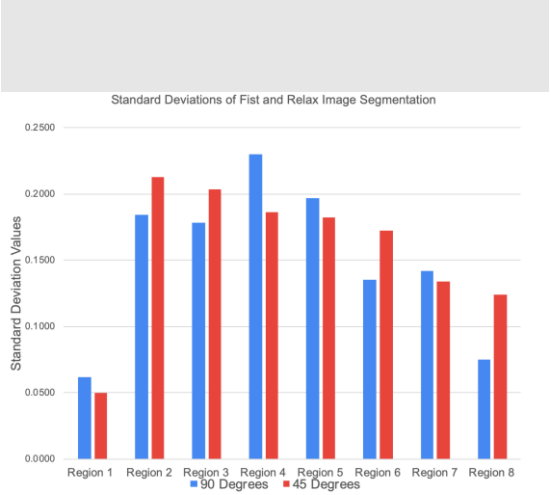
Standard Deviations of Fist and Relax Image Segmentation
Standard Deviation Values
Region 1
Region 2
Region 3
Region 4
Region 5
Region 6
Region 7
Region 8
90 Degrees
45 Degrees

Appendix C: Prosthetic Design Report

Introduction

In the prosthetic industry there are many different options to choose from. These products vary in material, size, function and appearance. This report investigates each of these aspects and more to determine which prosthetic features and qualities are needed for the Multi Degree of Freedom MQP prosthetic.

Background

Product Features

Through my research of many of the markets current and developing products I have been able to better understand the mechanical features of the prosthetic to best serve the needs of the consumer. These features can be broken down into material, mechanical design and lastly purpose served categories.

Material

PLA

One of the materials that regularly came up was PLA. PLA is an easy to print thermoplastic that tends to have a higher strength and stiffness than both ABS and nylon. With relatively low melting temperature and minimal warping, PLA is one of the easiest materials to 3D print successfully. There are variations of PLA that may better suit this project as some are more flexible and thus more impact resistant and better for added grip.

ABS

Another material option is ABS. ABS is a weaker and less rigid option relative to PLA but is also a tougher, lighter filament more suitable for some other applications. ABS is a bit more durable, 25% lighter, and has a four times higher impact resistance. ABS does however require more effort to print than PLA because it’s more heat resistant and prone to warping.

Nylon

Nylon is one of the other options that may fit our needs as it is a flexible, durable plastic. Its malleability lends it much more toughness than the other two, however, with an impact resistance ten times that of ABS. Nylon like the other two has many variations that can also better serve our specific needs.

Leather

Another material that came up within the prosthetic designs was leather. Leather was frequently used as the material to interface both with the patient and with the objects. The nature of leather being more similar to skin than plastic and also being flexible makes it a popular choice. One of the large downsides though is its cost to use. Relative to the other three, leather tends to be more expensive.

Mechanical Design

Actuation System

Current prosthetic designs have many different methods of control and moving the digits. The most popular two are cable and linkage systems. The cable systems function through attaching a cable to the end of the prosthetic fingers and running the cable through the digit and up the arm to the actuation control device. The other system is a linkage system which functions using a motor moving the finger at the base though the use of gears and is more simply able to control the flexion of the digits compared to each other to ensure the most realistic movement pattern.

Number of Finger Pieces

Across all the prosthetics on the market, whether to use two- or three-piece fingers varied greatly. Both sides of the argument are valid and understandable. Three-piece finger systems most closely resemble actual human hands as there is movement in the last phalanx. Though the movement is minimal and, in most cases, less than 10 degrees several designs feature the movement for its similarity to a human hand. The functionality though of this is limited. Other designs rather combine the two designs to one piece to create a connected medial and distal phalanx with a pre-set angle of rotation. This design reduces complexity and maintains nearly the same level of functionality. One variation on the two designs is the utilization of a spring in the last digit which could be used to apply a constant load at the tip while eliminating the need for a cable or linkage to connect to it. This active gripping force is something that is important to ensure that the motor doesn’t always have to be running.

Number of Motors

Across the designs on the market there is inconsistent practices with how many motors to use. These designs vary from one motor to 6. Each design varies with the level of control desired with the prosthetic. With each motor though, the cost increases. One of the designs featured 6 motors, one for each finger and an extra for the thumb to support a second axis of movement. Though this would allow the most realistic

movement track, it also nearly increased the price by 10% on the entire prosthetic. Other designs featured less motors which limited individual digit control in favor of affordability and simplified movement.

Purpose Served

Approximately 30 million people worldwide are in need of prosthetics. Each of these cases are unique with their own set requirements that the prosthetic can serve. With regards to arm prosthetics, the top priorities are to be able to function through day to day tasks. These include but aren't limited to getting dressed, daily hygiene, food and "simpler" tasks like opening a door. Each of these task require different movements and loads. Through a study conducted it was found that most of these tasks require one of three motions and are within the 2-8lb of force required region. This is the largest priority for most users, but other priorities are the discreetness, reliability and the customizability of the prosthetic.

Priorities List:

- Functionality
    - Must be able to complete day to day tasks
- Cosmetics
    - Patients desire products that don't stand out
- Weight
    - Patients must be able to support the prosthetic with ease
- Cost
    - Must be affordable for both project and customer
- Customizability
    - Must be able to fit a wide range of patients
- Durability
    - Must be made of durable materials that can withstand regular daily use
- Serviceability/Simplicity
    - Must not be too complex that it can't be adjusted and fixed with ease

Current Products

Current products on the market that are most similar to the purpose we are looking for include the following list.

1. Cyborg Beast
    a. Prioritize robustness for functionality
    b. Fixed thumb angle
    c. Metal fasteners are used for pins which is expensive
2. Talon Hand

    a. Uses leather instead of 3d print for human interface
    b. Offers choice of Chicago screw or snap pins
    c. Less plastic → More leather
3. Odysseus Hand
    a. Starter version of the Talon Hand
    b. 3 finger design
    c. Lower maximum load
4. Flexy Hand
    a. Most realistic design
    b. Uses filaflex filament which allows no elastics but is more expensive and complex
    c. Uses elbow movement to actuate
5. Flexy Hand 2
    a. Uses gauntlet instead of arm
    b. Uses less material
    c. Uses wrist to move
6. Raptor Hand
    a. Easy to assemble
    b. Almost completely 3d printable
    c. Bulky and exposed parts
7. Raptor Reloaded Hand
    a. Improved version of Raptor
    b. Recessed channels
    c. Less bulky
8. Dextrus Hand
    a. More degrees of freedom than most
    b. Two axis of motion for thumb
    c. Controlled electronically and uses steel cables, metal bearings and an internal pulley subassembly →↑Cost
9. Osprey Hand
    a. Easy to produce
    b. Utilizes leather
    c. Not easy to build
10. Phoenix Hand
    a. Easy to build due to instructions
    b. Uses small elastics that attach up the hand to fingers
    c. Fits on smaller sizes
11. K-1 Hand
    a. All 3D printed minus cables
    b. No instructions for assembly
    c. Organic shapes and possibly best looking

Analysis

Weighted Matrix

		Material			Number of Joints		Movement System		Number of Motors		
Priorities	Scaling Weight	ABS	Nylon	PLA	2	3	Linkage system	Cable system	6	5	<4
Weight	7	5	5	5	5	4	5	5	3	4	5
Max Load	9	5	5	5	7	6	7	4	7	6	5
Range of Motion	9	5	5	5	5	9	5	5	10	8	4
Cost	6	6	4	5	6	5	5	6	1	3	5
Assembly Time	5	5	5	5	6	3	6	5	3	4	6
Durability	8	5	6	5	6	4	5	5	3	5	7
Manufacturing Time	5	5	5	5	5	4	4	5	5	5	5
Gripping Ability	9	5	7	6	6	7	5	5	7	6	5
Scalability	8	5	5	5	5	5	4	6	5	5	5
Cosmetics	9	5	5	5	3	5	5	7	5	5	5
Reliability	10	5	5	5	6	4	5	5	4	5	6
Serviceability	10	5	5	5	6	4	6	5	4	5	6
Total		466	**480**	469	**504**	481	476	**483**	465	485	**488**

Conclusion

From the weighted matrix and information gathered through this research, the best material for our application is nylon, the optimal number of joints per finger is 2, the best motion system is cable, and the optimal number of motors is 4 which means one axis of motion for the thumb. With these determinations our team will be able to procced in making the proper modifications to the design to fit these requirements and future determinations that will be made in the coming days.

Determined Requirements

- Material: Nylon
- Finger Joints: 2
- Motion System: Cable
- Number of Motors: <4 (largely due to cost)
- Motion Pattern: Medial/Distal should angulate at same rate as proximal
- Desired Grasps Performed: Ball Grasp, Point, Fist, Open Palm
- Best Base Design: TBD
- Triggering System: TBD
- Cost: TBD
- Type of Motor: TBD

Future Improvements

- Multiple materials
- Grasp sensors
- Increased number of motors
- Active gripping aspect with all fingers

Appendix D: Prosthetic FEA

Hypothesis

When we test the index finger of the FlexyHand design with finite element modeling software, and correspondingly identify the force limits of the finger model, we will find that the design will be able to withstand loads that are greater than or equal to the force it will be projected to experience when in use and typing on a keyboard(25-180grams of force).

Methodology

Create the Model Parts

To begin the process, a model is required. This was created with each part of the finger meaning each segment was created individually and so was the hinge. These parts also needed to have similar dimensions because the hinge would be reused in joint. In the end, there were four separate part files that would be utilized in the assembly.

Create Model Assembly

This step builds off the previous one by taking all the parts and combining them into a single assembly. This was done by first creating a new assembly file.

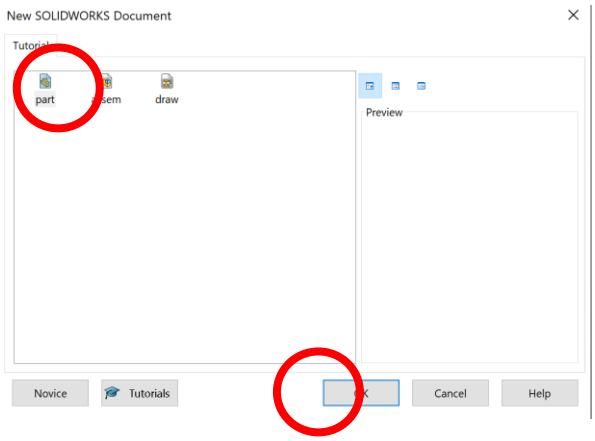

Figure 34: SolidWorks Assembly File Screen

Following that, the next step was to create all required mates. In this case, all the mates were from hinge to segment. This link can be used to find out more on mates and how to utilize them properly. These mates are important and must be accurate as to make sure the part reacts similarly to how it would

should it be physically produced. After creating all the mates, the visual should be a complete assembly like the image below.

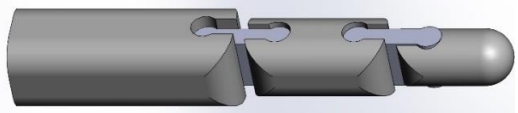

Figure 35: Finger Assembly Model

Create/Assign all Variable Values

Material

For this step, all parts must be assigned a material as to ensure it responds accurately to the simulation. In this analysis I had to create two new materials for PLA and Soft PLA as they are not default materials in SolidWorks. To do this I needed to research and gather the modulus of elasticity, Poisson's ratio, density, and yield strength. Each of these values then got plugged into the charts below. Both images show the values I used as well which can be used for future models.

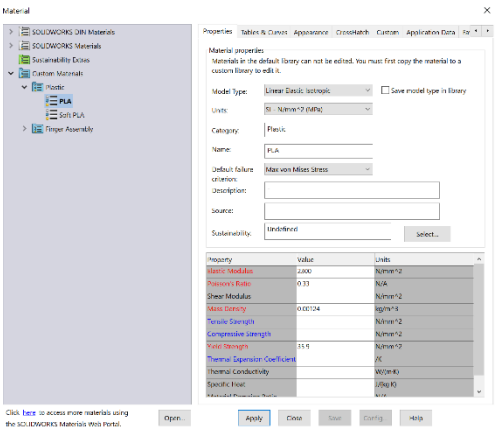

Figure 36: SolidWorks Material Selection/Creator Screen (PLA)

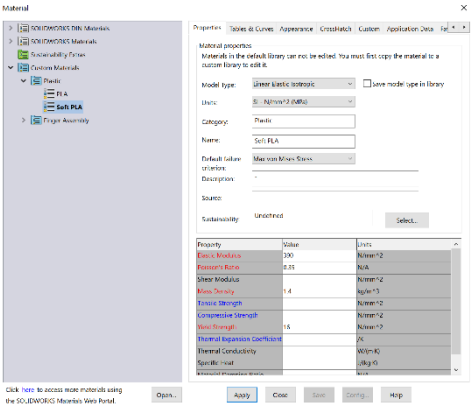

Figure 37: SolidWorks Material Selection/Creator Screen (Soft PLA)

Fixtures

This step involved ensuring the part is fixed in the right location so that we know it doesn't move freely when a load is applied. I applied the fixture to the base of the finger which can be shown in the image below with the green arrows.

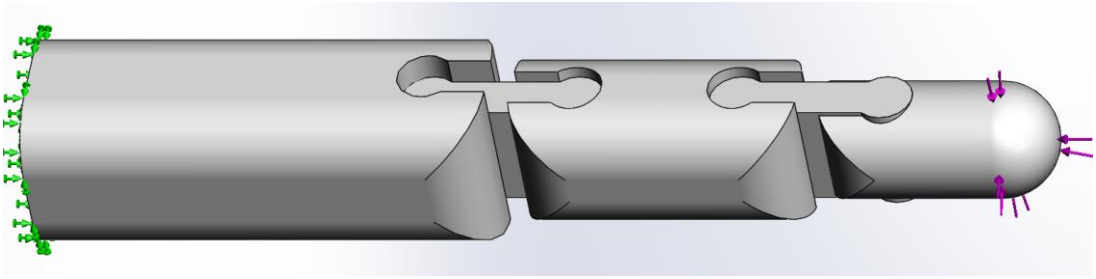

Figure 38: Finger Model Showing Fixture and Loading

Force

For this step I applied a loading in the location I believed would experience the load when typing. I chose half of the fingertip. This is don't by clicking on external loads and then force. This will produce this screen which you will populate. After selecting the location for the loading, you must input the value for the load. I did this with four different loads and had to repeat the entire study each time. Also, it is important to select the right units. The four loads I used should accurately reflect potential loads the finger will have to withstand. These loads were found through research on prior studies. I believe the lower loading values to be the most likely for typing based on my research but there is also a large amount of variability based on user and keyboard which is why the range was from 1N to 14.7N (1500g).

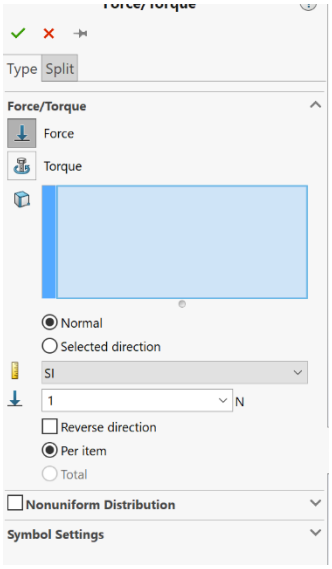

Figure 39: SolidWorks Force Loading Screen

Run SolidWorks Simulation Study

After the assembly is made and all the variables are complete, the next step is to run the study which is done by clicking the “Run This Study” button.

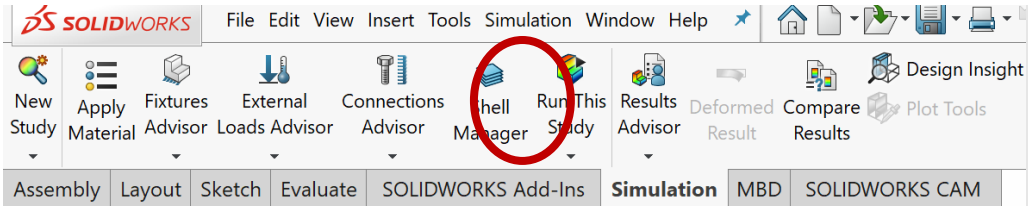

Figure 40: SolidWorks Simulation Taskbar

Conduct Further Analysis

After running the study, it will by default output visual representations of the stress, strain, and displacement. The representations can be seen in the findings section. These results are qualitative rather than quantitative and thus were lacking. In order to gather quantitative data, I conducted further testing by placing a “probe” on each face of the hinges under each of the loads and then downloaded the data points collected. These data points were then used to create box and whisker plots to show the distribution. I also created a table to call out the maximum values which are what is most important in understanding if the part fails.

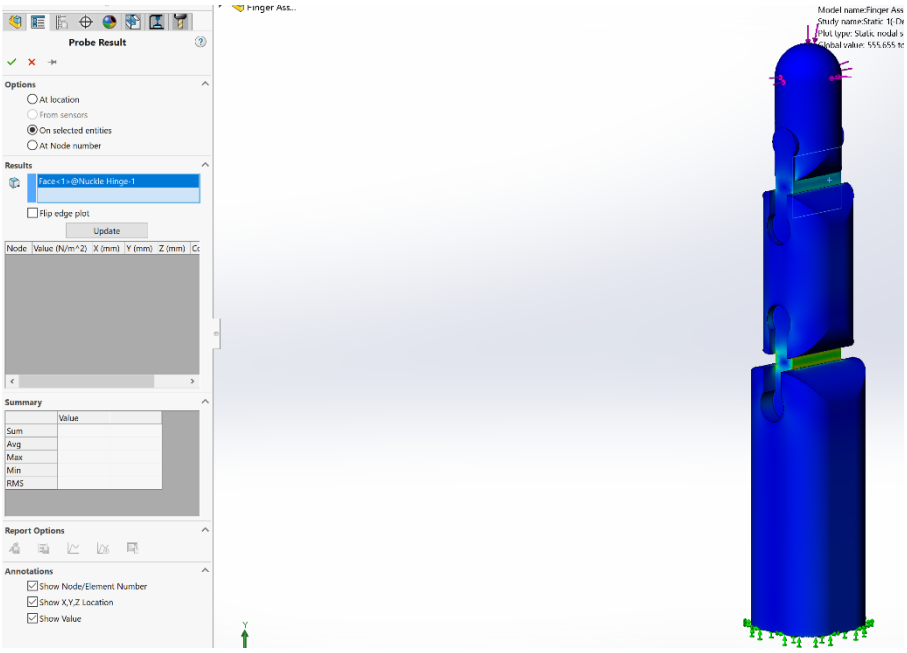

Figure 41: Probe Study Analysis

Review Results

The maximum values discovered in the above section are then compared to the found hypothetical yield strength to understand whether the part will fail.

Findings

Below are images that display the orientation of the finger model which can be referenced to better understand the data within the later figures.

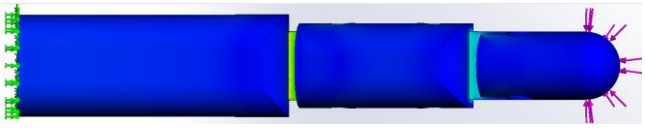

Figure 42: Stress Simulation Showing Model Stress (Exterior)

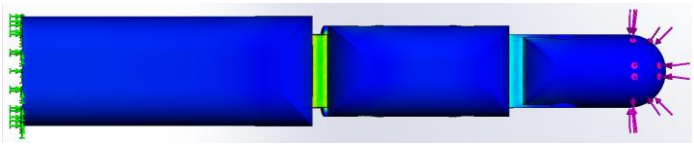

Figure 43: Stress Simulation Showing Model Stress (Interior)

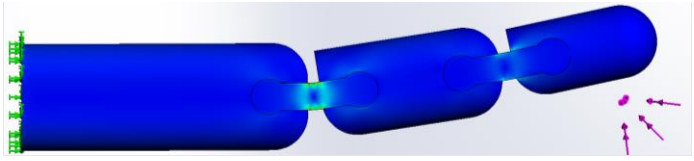

Figure 44: Stress Simulation Showing Model Stress (Side 1)

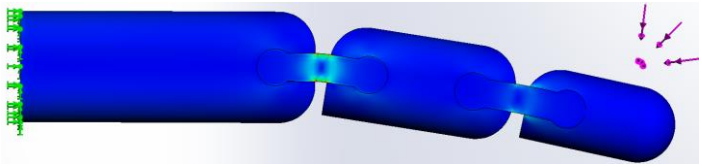

Figure 45: Stress Simulation Showing Model Stress (Side 2

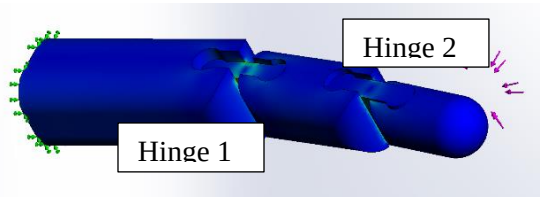

Figure 46: Stress Simulation Showing Model Stress (Isometric)

1N Applied Load

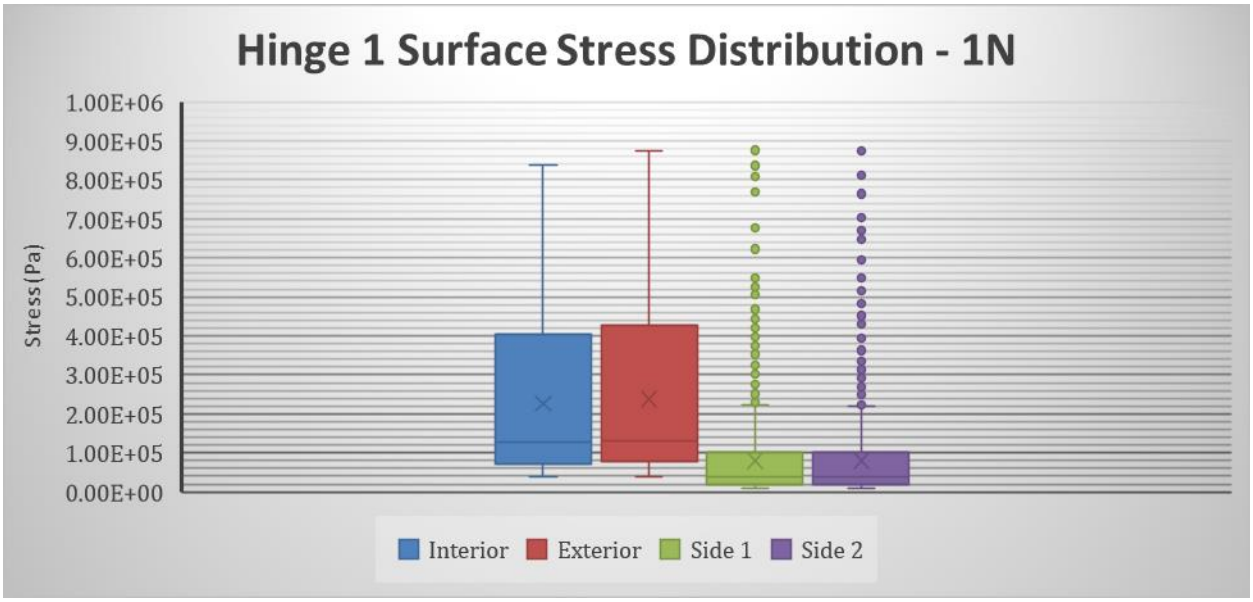

Figure 47: Hinge 1 Surface Stress

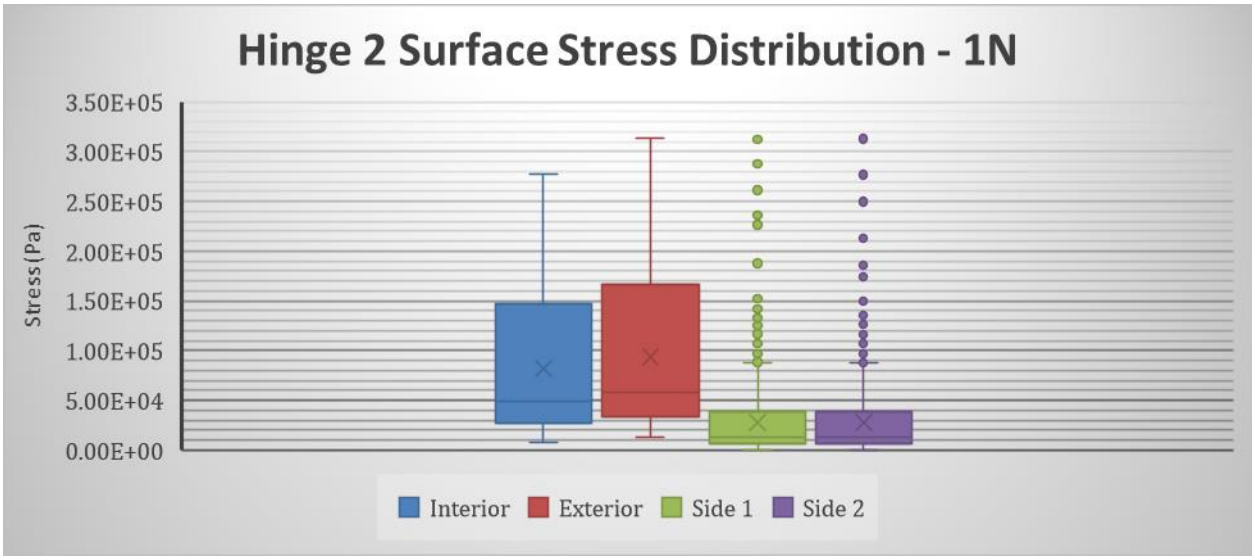

Figure 48: Hinge 2 Surface Stress

	Hinge 1				**Hinge 2**			
	Interior	**Exterior**	**Side 1**	**Side 2**	**Interior**	**Exterior**	**Side 1**	**Side 2**
MAX	8.36E+05	8.75E+05	8.75E+05	8.73E+05	2.77E+05	3.13E+05	3.12E+05	3.13E+05
MIN	3.93E+04	3.92E+04	7.82E+03	7.84E+03	7.78E+03	1.26E+04	2.81E+02	3.45E+02
Average	2.25E+05	2.37E+05	7.87E+04	7.91E+04	8.19E+04	9.36E+04	2.75E+04	2.75E+04

Table 6: 1N Surface Stress Values

500g Applied Load

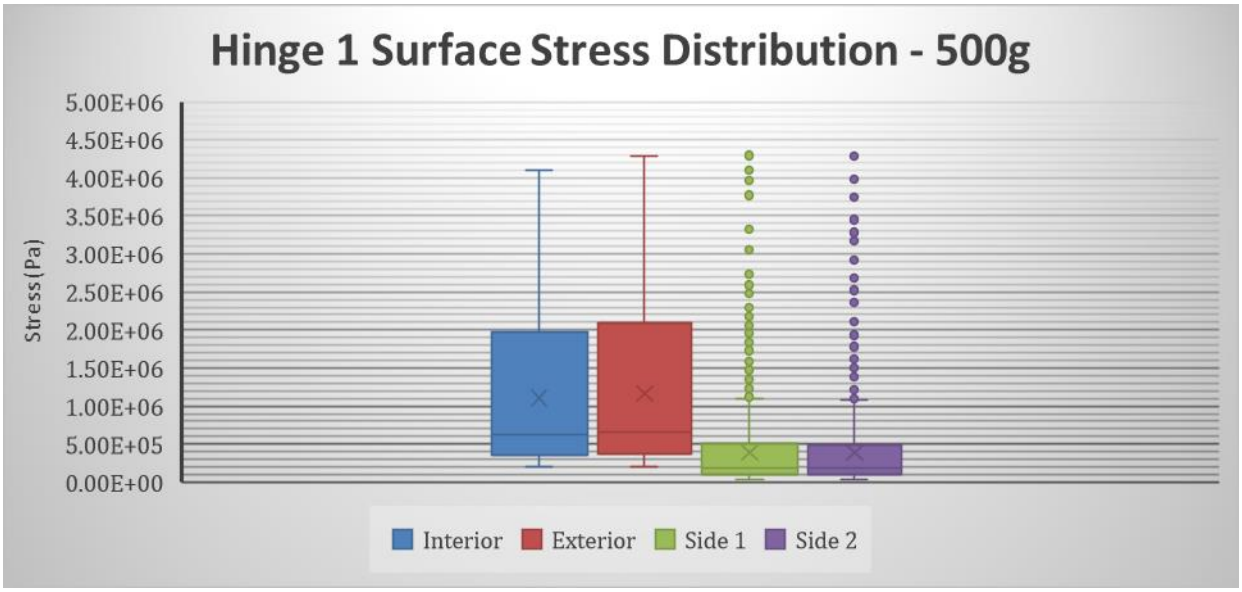

Figure 49: Hinge 1 Surface Stress

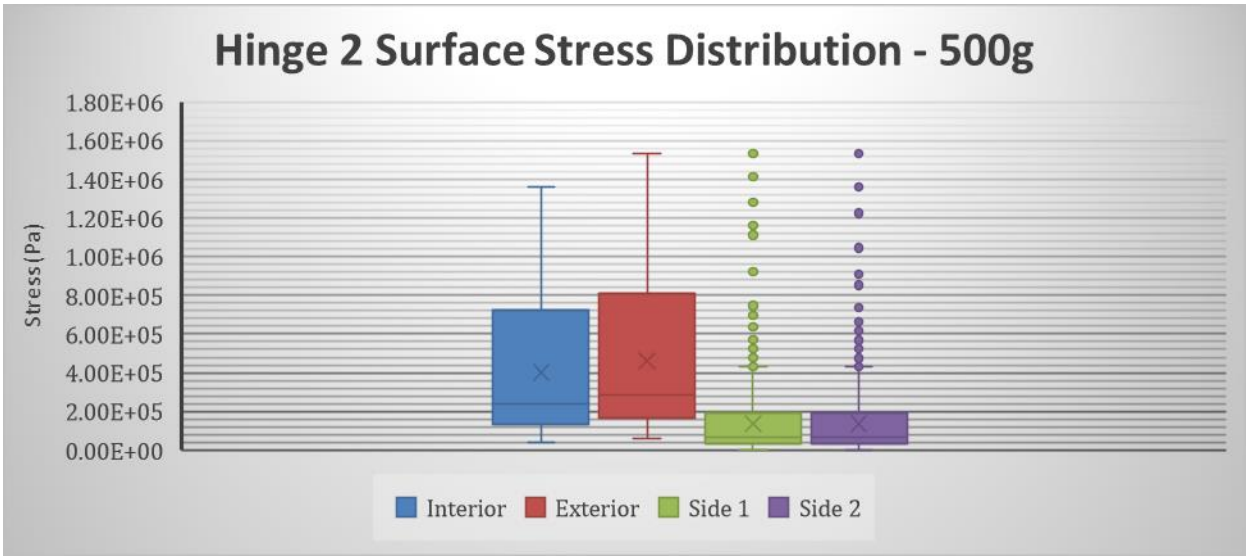

Figure 50: Hinge 2 Surface Stress

	Hinge 1				**Hinge 2**			
	Interior	**Exterior**	**Side 1**	**Side 2**	**Interior**	**Exterior**	**Side 1**	**Side 2**
MAX	4.10E+06	4.29E+06	4.29E+06	4.28E+06	1.36E+06	1.53E+06	1.53E+06	1.53E+06
MIN	1.93E+05	1.92E+05	3.84E+04	3.84E+04	3.81E+04	6.17E+04	1.38E+03	1.69E+03
Average	1.10E+06	1.16E+06	3.86E+05	3.88E+05	4.01E+05	4.59E+05	1.35E+05	1.35E+05

Table 7: 500g Surface Stress Values

1500g Applied Load

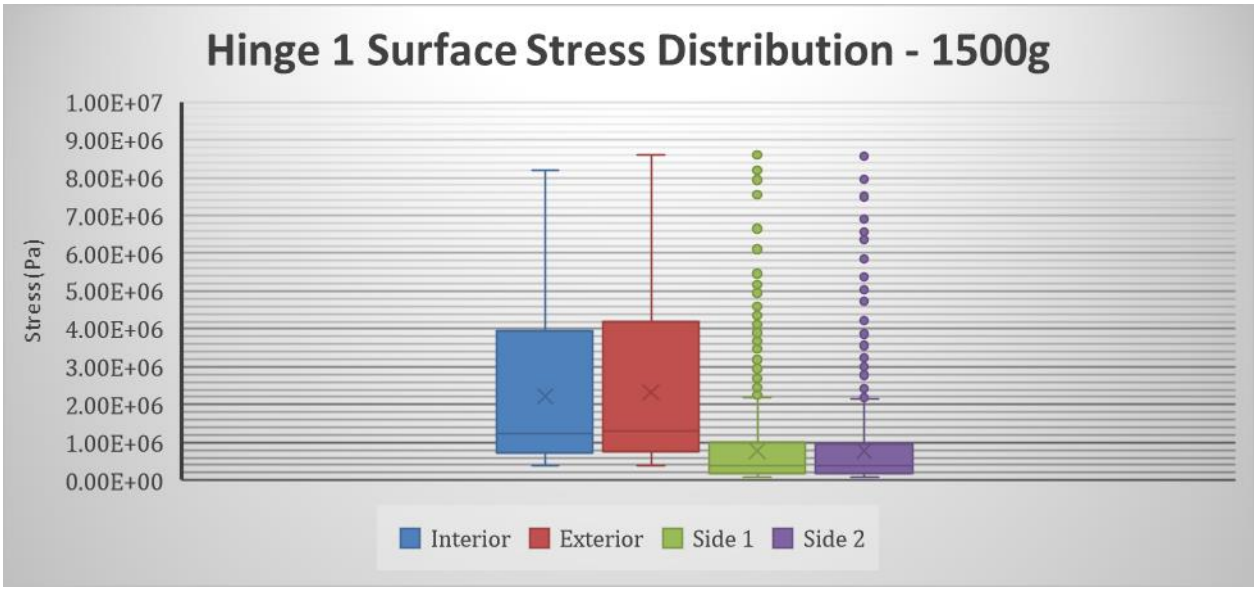

Figure 51: Hinge 1 Surface Stress

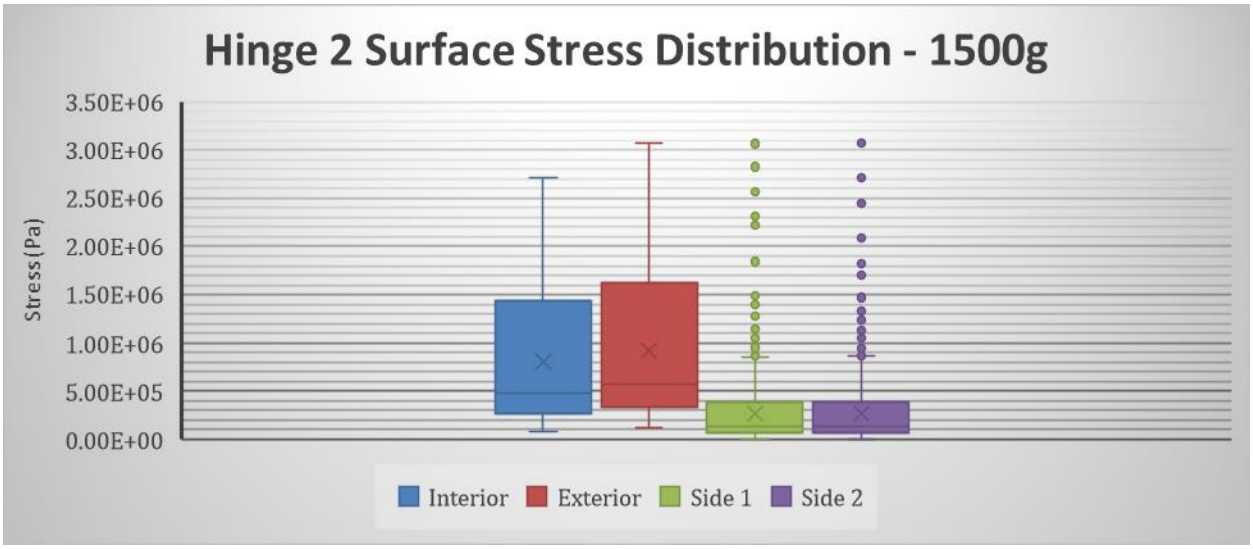

Figure 52: Hinge 2 Surface Stress

	Hinge 1				**Hinge 2**			
	Interior	**Exterior**	**Side 1**	**Side 2**	**Interior**	**Exterior**	**Side 1**	**Side 2**
MAX	8.20E+06	8.58E+06	8.58E+06	8.56E+06	2.71E+06	3.07E+06	3.06E+06	3.07E+06
MIN	3.85E+05	3.84E+05	7.67E+04	7.69E+04	7.63E+04	1.23E+05	2.75E+03	3.38E+03
Average	2.21E+06	2.32E+06	7.72E+05	7.76E+05	8.03E+05	9.18E+05	2.69E+05	2.69E+05

1000g Applied Load

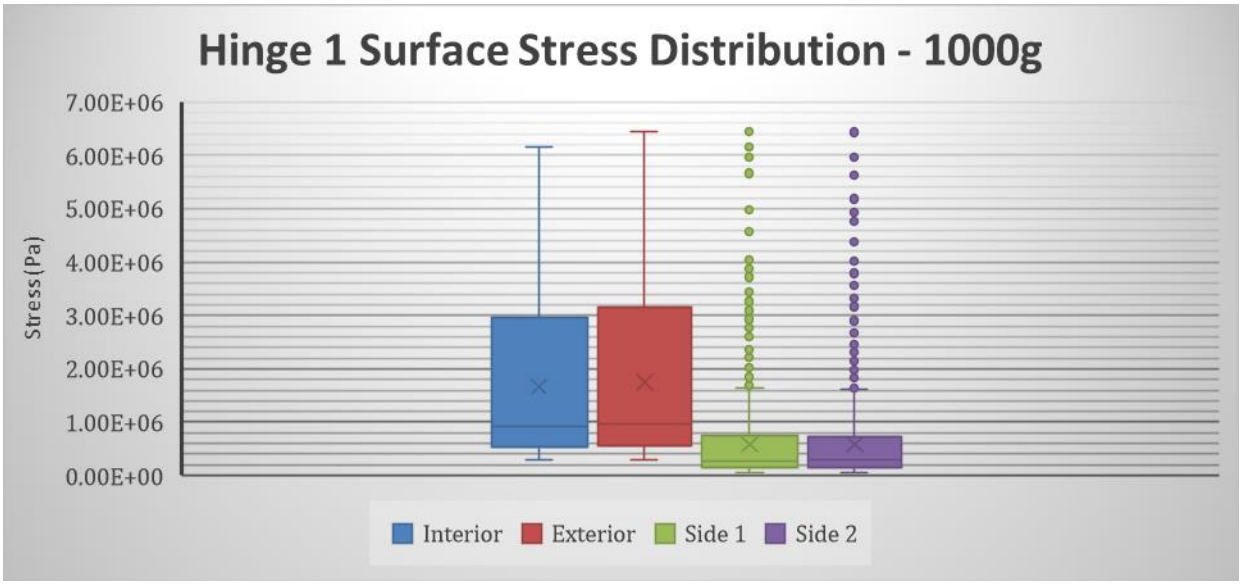

Figure 53: Hinge 1 Surface Stress

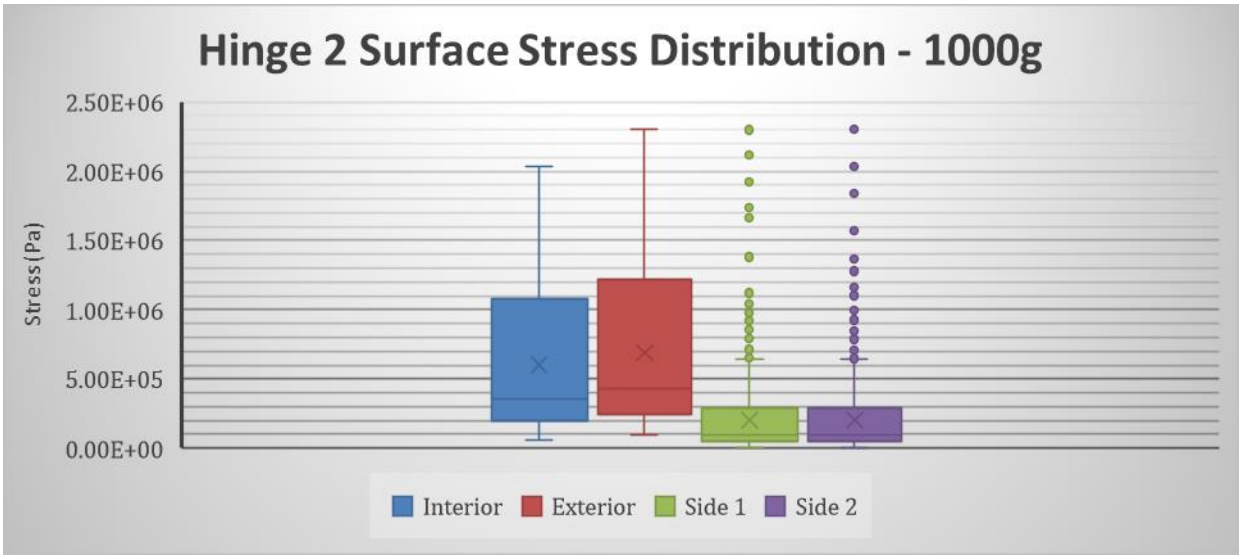

Figure 54: Hinge 2 Surface Stress

	Hinge 1				**Hinge 2**			
	Interior	**Exterior**	**Side 1**	**Side 2**	**Interior**	**Exterior**	**Side 1**	**Side 2**
MAX	6.15E+06	6.44E+06	6.44E+06	6.42E+06	2.04E+06	2.30E+06	2.30E+06	2.30E+06
MIN	2.89E+05	2.88E+05	5.75E+04	5.77E+04	5.72E+04	9.26E+04	2.07E+03	2.54E+03
Average	1.66E+06	1.74E+06	5.79E+05	5.82E+05	6.02E+05	6.88E+05	2.02E+05	2.02E+05

Summary

From the data collected I was able to extrapolate the maximum stress experienced with each load amount. I found them to be .875MPa, 4.29MPa, 6.44MPa, and 8.58MPa for the 1N, 500g, 1kg, and 1.5kg loads respectively. When I compare these values to the material properties of soft PLA, which is the material utilized in the tested region, I found these values to be lower than the 16MPa yield strength.

Conclusion

From my findings I was able to support my hypothesis. This is because the maximum probable stress due to loading is lower than the yield strength of the material being used in the highest loaded regions.

Recommendations

From this conclusion my recommendation would be that this design is suitable for this application using these materials. If any further changes are required, then a follow-up FEA should be conducted as to ensure the materials and design can support the potential loads for the applications.